



Biogeochemical versus Conventional Landfill Soil Covers: Analysis of Gas Flow Profiles, Microbial Communities, and Mineralogy

Jyoti K. Chetri, S.M.ASCE¹; Krishna R. Reddy, F.ASCE²; Dennis G. Grubb, M.ASCE³; and Stefan J. Green⁴

Abstract: In this study, a novel biogeochemical cover system comprising biochar-amended soil and basic oxygen furnace (BOF) steel slag was explored as a sustainable alternative cover system to mitigate methane (CH₄), carbon dioxide (CO₂), and hydrogen sulfide (H₂S) simultaneously from landfill gas (LFG). Long-term column studies of a simulated biogeochemical cover (BGCC) profile investigated CH₄, CO₂, and H₂S removal potential. The performance of the BGCC system was compared with a conventional soil cover (SC) profile. The CH₄ oxidation rates of biochar-amended soil were significantly higher, ranging from 185 to 407 μg CH₄/g-day in comparison with the barrier soil in the SC system (6–7.5 μg CH₄/g-day), based on the batch incubation of column-exhumed samples. In addition, the biochar-amended soil showed higher relative abundance of methanotrophic bacterial communities (20%–51%) in comparison with soil cover (10%–27%). In both columns, complete attenuation of H₂S occurred near the inlet (75 cm bgs) and sulfur oxidizing bacteria (e.g., *Thiobacillus*) and methanotrophs were both detected. The sulfur content was elevated (0.68%) at the base of both columns and H₂S may have imparted an inhibitory effect on CH₄ oxidation rate in the SC system. The BOF slag showed a CO₂ removal potential of 67 g CO₂/kg BOF slag. Overall, the BGCC system outperformed the SC system, effectively mitigating CH₄, CO₂, and H₂S simultaneously. **DOI:** 10.1061/(ASCE)HZ.2153-5515.0000708. © 2022 American Society of Civil Engineers.

Author keywords: Alternative cover; Biogeochemical cover; Biochar amended; BOF slag; Soil conventional soil cover.

Introduction

Landfill gas (LFG) comprises approximately 50% methane (CH₄), 50% carbon dioxide (CO₂) with minor amounts of some nonmethane organic compounds (NMOCs) (USEPA 2021). In the United States, municipal solid waste (MSW) landfills are regulated under Subtitle D of the Resource Conservation and Recovery Act (RCRA). As per Subtitle D requirements, the final cover must include an infiltration layer of earthen material with a minimum thickness of 18 in. (\sim 45 cm) and an overlying erosion protection layer of earthen material with a minimum thickness of 6 in. (\sim 15 cm).

Unfortunately, MSW landfills are the third largest source of CH₄ emissions in the United States (USEPA 2021). Three engineered controls have been found to be highly effective in mitigating landfill CH₄ emissions: (1) gas collection and recovery systems; (2)

Note. This manuscript was submitted on December 8, 2021; approved on March 10, 2022; published online on May 16, 2022. Discussion period open until October 16, 2022; separate discussions must be submitted for individual papers. This paper is part of the *Journal of Hazardous, Toxic, and Radioactive Waste*, © ASCE, ISSN 2153-5493.

physical barriers of engineered cover materials; and (3) microbially mediated CH₄ oxidation (Bogner et al. 2011). Extensive efforts have been made to enhance the microbial CH₄ oxidation potential of landfill cover soils, including the addition of organic-rich materials such as compost, peats, garden waste, and biochar (Sadasivam and Reddy 2014; Chetri and Reddy 2021; Reddy et al. 2021). Biochar-amended soils have shown promise for enhancing the CH₄ oxidation potential of the landfill cover soil (Yargicoglu and Reddy 2018; Reddy et al. 2021). Biochar, a solid carbonaceous product derived from biomass (waste), has unique properties such as resistance to degradation, high moisture retention, high microporosity and specific surface area, and gas absorption potential, which makes it attractive for CH4 oxidation applications (Sadasivam and Reddy 2015; Xie et al. 2015; Yargicoglu et al. 2015). Compost-based biocovers have shown notable reductions in CH₄ via biodegradation (Scheutz et al. 2009; Scheutz and Kjeldsen 2005). Similarly, Ding et al. (2019) investigated a biochar-sludge compost combination for odor removal. However, no study has focused on the removal of CH4, CO2, and hydrogen sulfide (H₂S) by cover systems incorporating biochar.

Recently, a layered biogeochemical cover (BGCC) system with biochar-amended soil and basic oxygen furnace (BOF) steel slag was explored for simultaneous removal of CH₄, CO₂, and H₂S (Chetri et al. 2019). Biochar-amended soil can mitigate CH₄ emissions by microbial methane oxidation (Yargicoglu and Reddy 2017a, b, 2018). Sand-sized BOF steel slag particles can mitigate CO₂ and H₂S emissions through carbonation and sulfidation reactions (Chetri et al. 2019, 2020). Recent column studies simulating three different profiles of a biogeochemical cover system (BOF slag underlain by biochar-amended soil layer) showed strong potential for CH₄, CO₂, and H₂S removal under simulated landfill conditions (Chetri et al. 2022b). In a prior study (Chetri et al. 2022a), 5% methanotrophically activated biochar-amended soil was found to be optimal but sustaining methanotrophic bacterial consortium on

¹Graduate Research Assistant, Dept. of Civil, Materials, and Environmental Engineering, Univ. of Illinois at Chicago, 842 West Taylor St., Chicago, IL 60607. Email: jkc4@uic.edu

²Professor, Dept. of Civil, Materials, and Environmental Engineering, Univ. of Illinois at Chicago, 842 West Taylor St., Chicago, IL 60607 (corresponding author). ORCID: https://orcid.org/0000-0002-6577-1151. Email: kreddy@uic.edu

³President, Fugacity LLC, 324 Broadway Ave., West Cape May, NJ 08204. Email: dggrubbphdpe@gmail.com

⁴Director, Genomics and Microbiome Core Facility, Rush Univ. Medical Center, 1750 W. Harrison, Jelke Building, Room 444, Chicago, IL 60612. ORCID: https://orcid.org/0000-0003-2781-359X. Email: stefan_green@rush.edu

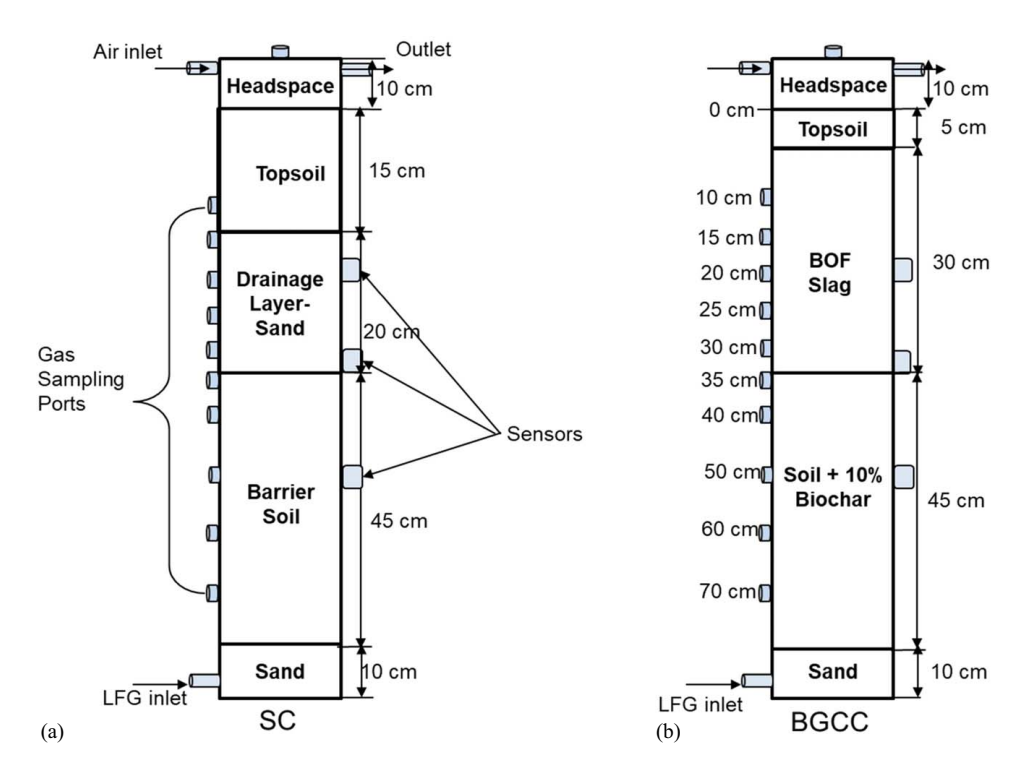


Fig. 1. Schematic of the cover profiles in the column testing: (a) SC; and (b) BGCC

a large scale for field application may be a challenge. Accordingly, this study focused on evaluating the performance of nonactivated biochar-amended soil as a component of biogeochemical cover systems and to: (1) compare the gas removal efficiency and microbial activity of BGCC and soil cover (SC) systems under dynamic gas flow conditions; (2) evaluate the system performance as BOF slag carbonates; and (3) investigate the effect of environmental factors such as rainfall on the performance of simulated cover systems.

Materials and Methods

Column Setup and Source Material Characterization

To approximate field conditions for experimental testing, simulated cover profiles were created with soil columns. The RCRA Subtitle D cover profile was simulated using a conventional SC profile, as shown in Fig. 1. The column, from bottom to top, consisted of a sand gas distribution layer (GDL), a barrier soil layer, a sand drainage layer, and a topsoil vegetative soil layer. Similarly, a simulated BGCC column was created, with a profile consisting of a sand GDL, a 10% (w/w) biochar-amended soil layer, a BOF slag layer, and a topsoil layer (Fig. 1). Ottawa (20/40) sand (US Silica, IL, USA) was used for the GDL and drainage layers. Landfill cover soils were obtained from different locations from the intermediate cover of the Zion landfill (Zion, IL). Soil with higher fines content (90.2%) was used in the barrier layer in the SC as the purpose of the barrier soil in real practice is to minimize infiltration and requires low hydraulic conductivity (K). Soils with high fines content result in low K. Soil with relatively lower fines content (81.7%) and higher organic content (3.6%) was used for the topsoil layer in both profiles. Soil with the lowest fines content was used in the biochar-amended soil layer in the BGCC column. Pinewood-derived biochar (Chip Energy, IL, USA) was used. The BOF slag was obtained from Indiana Harbor East Steel Mill, East Chicago, IN.

The physical, chemical, and geotechnical parameters of the landfill cover materials and associated testing methods are summarized in Table 1. The *K* of the barrier soil, topsoil, and 10% biocharamended soil were determined as per ASTM D5084 (ASTM 2016) in a flexible wall permeameter using samples with the same density as the column samples. The *K* of sand and BOF slag were measured as per ASTM D2434 (ASTM 2019b) in a constant head permeameter. The pH of the soils was measured using an Orion 720A pH meter (Thermo Scientific Orion 0720A7, Fisher Scientific, UK). Carbonate content testing was performed using a portable calcium carbonate content chamber (HM-4501, Humboldt Mfg. Co., USA) as per ASTM D4373 (ASTM 2021b).

To create soil columns, the soils were placed in plexiglass tubes (100 cm high and 18.40 cm inside diameter) using the placement procedures outlined in Yargicoglu and Reddy (2018) (Fig. 1). The inlet gas and inflow rates to the sand GDL were regulated through a flowmeter and manifold system. Sampling ports were installed at multiple elevations. Gas sampling ports in the upper 50 cm of the column were spaced at 5 cm and the bottom 50 cm were spaced at 10 cm apart. A gas sampling port was located at the top cap of the column to measure headspace gas concentrations. Time-domain reflectometry (TDR) sensors (CS655-L, Campbell Scientific, Logan, Utah) were emplaced at three locations [20, 35, and 50 cm below top (ground) surface] and temperature, volume water content (VWC), and electrical conductivity (EC) were measured and recorded continuously by a data acquisition system (Campbell Scientific CR1000 Data Logger equipped with an AM16/32 B multiplexer, Campbell Scientific, Logan, Utah). To simulate air movement above the SC, atmospheric air was passed through a water column and fed in the column from the top left side. A digital mass flowmeter was connected to the outlet of the column to measure outflowing gas rates. A sampling port was positioned in the top cap of each column to measure headspace gas concentrations.

In each column, a 10-cm thick dry sand layer (GDL) was loosely placed by air pluviation. In the SC column [Fig. 1(a)], a 45-cm

Table 1. Properties of the cover components used in the column tests

Properties	ASTM method	Barrier soil-SC	Drainage sand	Soil-BGCC	BOF slag	Topsoil
Specific gravity	ASTM D854 ASTM (2014)	2.72	2.66	2.65	3.34	2.59
Organic content/loss on ignition (%)	ASTM D2974, ASTM (2020)	2.0	0.3	4.9	1.94	3.6
Grain size distribution						
Gravel (%)	ASTM D6913/6913M, ASTM (2017a)	0.0	0.0	0.0	0	0.2
Sand (%)	_	9.8	100	35.4	86.4	18.1
Fines (%)	<u> </u>	90.2	0.0	64.6	13.6	81.7
D ₅₀ (mm)	_	0.007	0.6	0.023	0.82	0.018
C_c	_	_	0.91		29.17	_
C_u	_	_	1.36		0.72	_
Water holding capacity (% w/w)	ASTM D2980, ASTM (2017b)	56.5	27.8	46.1	29.6	47.5
Hydraulic conductivity (cm/s)	ASTM D5084 ASTM (2016)/D2434	1.3×10^{-7}	1.4×10^{-2}	ND	2.6×10^{-3}	1.8×10^{-7}
	ASTM (2019b)					
@dry density	<u> </u>	$@1.56 \text{ g cm}^{-3}$	$@1.6 \text{ g cm}^{-3}$		$@1.7 \text{ g cm}^{-3}$	$@1.30 \text{ g cm}^{-3}$
Moisture density relationship						
Maximum dry density (g/cm ³)	ASTM D698, ASTM (2021a)	1.80	ND	ND	ND	1.81
Optimum moisture content (%)	_	17.0	_	_	_	17.10
рН	ASTM D4972, ASTM (2019a, c)	7.9	6.7	8.0	12.4	7.7
Carbonate content (CaCO ₃ , %)	ASTM D4373, ASTM (2021b)	23.21	2.15	13.60	3.79	3.67

Note: Hydraulic conductivity test samples were prepared at densities similar to the layers placed in column reactors. Hydraulic conductivity and water holding capacity of 10% biochar-amended soil were 1.1×10^{-5} cm/s @ 1.21 g/cm³ dry density and 55.3%, respectively.

Table 2. Properties of the soil layers during placement in the column

	SC			BGCC				
Property	Barrier	Drainage	Topsoil	Biochar soil	BOF	Topsoil		
Bulk density (g/cm ³)	1.80	1.76	1.50	1.38	1.80	1.56		
Dry density (g/cm ³)	1.57	1.76	1.30	1.20	1.64	1.34		
Moisture content (%w/w)	15.0	0.0	15.0	15.0	10.0	16.0		
Void ratio	0.74	0.51	0.99	1.03	1.02	0.93		
Porosity (%)	42	34	50	51	50	48		

thick barrier soil layer, adjusted to a moisture content (MC) of 15%, was then placed in 5 cm lifts compacted with a tamping rod (3.1 kg) to a bulk density of 1,800 kg/m³. All soil layer boundaries were demarcated by a 6-oz (~170 g) needle punched geotextile fabric (EPI, Traverse City, MI). A 20-cm thick dry sand drainage layer was loosely placed on top of a barrier soil layer. Similarly, a 15-cm thick topsoil layer (adjusted to MC of 15%) was placed on top of a drainage sand layer in 5 cm lifts with light compaction. For the BGCC column [Fig. 1(b)], a 45-cm thick 10% (w/w) biocharamended soil layer was placed on top of the GDL. The biocharamended soil was mixed thoroughly in the dry state and adjusted to MC of 15% before placement. A 30-cm thick BOF slag layer at 10% MC was placed over the biochar-amended soil layer in 5-cm lifts with light compaction. Lastly, a 5-cm thick topsoil layer was placed on top of the BOF slag layer similar to the SC column. The engineering parameters of each column layer are summarized in Table 2.

Column Testing Phases

Each cover profile was exposed to LFG in four phases as summarized in Table 3. First, the columns were preincubated with a gas mixture containing 1,000 ppm CH₄ in 99.99% N₂. Each cover profile was exposed to approximately 0.2 g CH₄/m²-day for nearly 17 days to allow microbial communities to acclimate to column conditions. CH₄, CO₂, and O₂ concentrations were monitored every 2–3 days for CH₄ oxidation activity. On day 18, the

inlet gas composition was switched to 48.25% $\rm CH_4$, 50% $\rm CO_2$, and 1.75% $\rm H_2S$ for the next three phases at varying flow rates. Phases II and IV simulated low $\rm CH_4$ fluxes (50 g $\rm CH_4/m^2$ -day) whereas Phase III simulated a high $\rm CH_4$ flux (150 g $\rm CH_4/m^2$ -day). Each phase was operated until no significant changes in gas profiles were observed at depth (i.e., steady state conditions). In Phase III, rainfall was simulated by adding 340 mL (0.5 in.) of water to the top of the column after 20 days of Phase III operation.

 ${\rm CH_4}$, ${\rm CO_2}$, and ${\rm O_2}$ concentrations were monitored regularly using a gas chromatograph (SRI GC, Torrance, CA, USA) equipped with a thermal conductivity detector (TCD) for ${\rm CH_4}$ and ${\rm CO_2}$ detection, and a flame ionization detector/flame protonation detector (FID/FPD) for detection of ${\rm H_2S}$. The TCD was also used for detection of ${\rm O_2}$, with the carrier gas switched from helium to nitrogen.

Column Exhumation and Terminal Material Characterization

The column experiments were terminated after 176 days of operation, and subsamples were collected at various depths for physical, chemical, and microbial characterization. All samples were characterized for MC, organic content/loss on ignition (OC/LOI), pH, and carbonate content (Table 4). Subsamples extracted from barrier soil layer, biochar-amended soil layer, and topsoil layers were stored at -20°C for cultivation-independent molecular characterization, and at 4°C for batch incubation studies. Barrier and biochar-amended soils obtained at depths of 40, 50, 60, and 70 cm below ground surface (bgs) and BOF slag obtained from 15 and 35 cm bgs were analyzed for total carbon and sulfur content using an Eltra CS800 Analyzer consisting of an induction furnace and a tuned infrared detector by Pittsburgh Mineral & Environmental Technology, Inc (PMET). Details of the analysis are presented in Chetri et al. (2022b).

Batch Testing

All soil samples exhumed from barrier soil and biochar-amended soil layers were incubated in batch microcosms to measure potential CH₄ oxidation rates. Topsoil samples obtained at depths of 5 cm were also subjected to batch incubation. The batch

Table 3. Column exposure phases and flow conditions

			Flowrate	Opera wrate Avg. CH ₄ flux			
Phase	Description	Inlet gas	(mL min ⁻¹)	$(g CH_4 m^{-2} day^{-1})$	Start	End	Total duration (days)
I	Preincubation	1,000 ppm CH ₄ , 99.99% N ₂	5.3	0.2	0	17	17
II	Low flux	48.25% CH ₄ , 50% CO ₂ , 1.75% H ₂ S	2.8	50	18	43	26
III	High flux		9	150	44	102	59
IV	Low flux		2.8	50	103	176	74

Note: Phases II, III, and IV had same gas composition.

Table 4. Summary of initial and final soil parameter of cover soils

		MC (%)		OC/LOI (%)		рН		Carbonate content (CaCO ₃ , %)	
Depth bgs (cm)	Layer	I	F	I	F	I	F	I	F
SC									
5	Topsoil	16	19.4	3.6	2.2	7.7	8.22	3.67	3.24
10	Topsoil		19.0	_	2.8	_	8.29	_	3.67
15	Topsoil	_	18.9	_	3.0	_	8.32	_	3.94
16	Drainage sand	0	0.4	0.3	0.3	6.7	6.51	2.15	2.70
33	Drainage sand	_	0.2	_	0.4	_	6.32	_	1.51
40	Barrier soil	15	14.6	2.0	1.8	7.9	8.1	23.21	23.75
45	Barrier soil	_	14.8	_	1.8		8.07	_	21.70
55	Barrier soil ^a	_	14.5	_	1.8	_	8.0	_	24.56
65	Barrier soil	_	14.5	_	1.8	_	8.06	_	22.02
75	Barrier soil	_	15.0	_	2.0	_	7.32	_	17.81
85	GDL sand	0	0.1	0.3	0.4	6.7	6.18	2.15	2.16
BGCC									
5	Topsoil	16	23.3	3.6	3.7	7.7	8.39	3.67	3.29
10	Steel slag	10	11.4	1.94	2.3	12.3	11.74	3.79	15.44
15	Steel slag	_	11.5	_	2.4		11.49	_	16.09
25	Steel slag	_	12.3	_	2.5		11.31	_	16.73
35	Steel slag ^a	_	12.7	_	2.4	_	11.49	_	18.95
40	Soil + biochar	15	16.7	13.9	11.6	7.18	7.6	12.14	13.49
45	Soil + biochar	_	17.6	_	12.1	_	7.7	_	14.14
55	Soil + biochar	_	17.0	_	11.2	_	7.68	_	11.98
65	Soil + biochar	_	16.3	_	12.4	_	7.5	_	11.34
75	Soil + biochar ^a	_	15.1		7.5		7.25		11.61
80	GDL sand	0	0.3	0.3	0.5	6.7	6.57	2.15	2.54
90	GDL sand	_	0.1	_	0.6	_	6.28	_	1.78

Note: I = Initial and F = Final.

incubations were performed in triplicate using procedures as outlined in Chetri et al. (2022a). Briefly, approximately 10 g samples were placed in a sealable 125 mL glass serum vial. After sealing, 20 mL of air from the headspace was withdrawn and replaced by an equal volume of 50% CH₄ and 50% CO₂ to obtain starting headspace concentrations of ~6% CH₄ and 6% CO₂ balanced in air. Headspace gas concentrations were monitored regularly until the CH₄ concentration stabilized. CH₄ oxidation rates were calculated from CH₄ concentration versus time plots following zero-order kinetics (Yargicoglu and Reddy 2017a).

Batch tests were performed in triplicate on the carbonated BOF slag samples obtained from various depths (1, 10, 20, and 30 cm, below top of slag layer) to measure residual carbonation potential. For each test, approximately 1 g (dry weight) of carbonated BOF slag was placed in a 125 mL glass serum vial. Vials were purged with a 50% CH₄ and 50% CO₂ gas mixture, then sealed with rubber septa and aluminum crimps. Headspace concentrations of CH₄ and CO₂ were monitored to determine the residual CO₂ uptake/removal potential of the carbonated BOF slag.

XRD and SEM/EDS Analysis

Mineralogy was evaluated by performing X-ray powder diffraction (XRD) and Rietveld quantification analyses on the carbonated samples from the BOF slag (obtained from 35 cm bgs), biocharamended soil (obtained from 75 cm bgs), and barrier soil (obtained from 55 cm bgs) at PMET (Pittsburgh, PA, USA) as summarized in Table 5. Quantitative XRD (QXRD) analysis was performed on the samples following a similar procedure as explained in Reddy et al. (2019).

Select BOF slag samples, barrier soil samples, and biocharamended soil samples were analyzed with scanning electron microscopy (SEM) using a JEOL JSM-IT500HR high-resolution scanning microscope operated at 5.0 kV with a secondary electron detector (SED) for imaging. Energy dispersive spectrometry (EDS) analysis was performed using an Ultim Max, Oxford X-ray energy dispersive spectrometer operated at 20 or 30 kV. Sample preparation details for SEM analysis have been described previously (Reddy et al. 2019).

^aSample mineralogy evaluated (see Table 5).

Table 5. Mineralogical characterization of the column substrates after termination

Compound	Formula	SC barrier soil 55 cm	BGCC biochar soil 75 cm	BGCC BOF slag 35 cm	Fresh BOF slag
Quartz	SiO_2	31.2	37.2		_
Dolomite	$CaMg(CO_3)_2$	27.2	30.1	_	
Calcite	CaCO ₃	4.8	2.1	13.6	0.43
Muscovite	$KAl_3Ai_3O_{10}(OH)_2$	14	9.6	_	_
K-feldspar	KAlSi ₃ O ₈	10.9	8.3	_	
Plagioclase	(Na,Ca)(Si,Al) ₄ O ₈	8.6	9.1	_	
Clinochlore	Mg ₅ (Al,Fe)(Si, Al) ₄ O ₁₀ (OH) ₈	3.3	2.2	_	_
Pyrite	FeS ₂	_	0.6	_	_
Gypsum	CaSO ₄ -2H ₂ O	_	0.8	_	
Lime	CaO	_	_	1.2	1.76
Portlandite	$Ca(OH)_2$	_	_	_	4.67
Brownmillerite	$Ca_2Fe_2O_5$	_	_	20.9	17.41
Larnite	Ca ₂ SiO ₄	_	_	17.3	16.44
Magnesium iron oxide	(Mg,Fe)O	_	_	12.7	9.58
Wuestite	FeO	_	_	0.9	9.19
Magnesioferrite	$MgFe_2O_4$	_	_	8.7	7.79
Iron	Fe	_	_	0.2	_
Mayenite	$Ca_{12}Al_{14}O_{33}$	_	_	1.3	
Amorphous	noncrystalline	_	_	23.2	30.7

Microbial Analysis

Microbial community characterization was performed using DNAbased 16S ribosomal RNA (rRNA) gene amplicon next-generation sequencing (NGS), as described previously (Chetri et al. 2022a). Quantitative analysis of bacterial 16S rRNA gene abundance in DNA samples (e.g., Nadkarni et al. 2002) was performed using real-time quantitative PCR (qPCR), as described previously (Chetri et al. 2022a). Samples obtained from the topsoil, barrier soil, and biochar-amended soil at 5, 40, 45, 55, 65, and 75 cm bgs were processed in triplicate using both 16S rRNA gene amplicon sequencing and qPCR. Library preparation, sequencing and qPCR were performed by Genome Research Core (GRC) at the University of Illinois at Chicago (UIC). More detailed procedures for amplicon sequencing and qPCR are outlined in Chetri et al. (2022a). A basic annotation of sequence data was performed using a QIIME2 pipeline (Bolyen et al. 2019), as implemented previously (Chetri et al. 2022a) by the Research Informatics Core (RIC) at UIC.

Statistical Analysis

Statistical analyses of microbial taxa abundance in microcosm and column samples were performed using one-way ANOVA and *t*-tests (equivalency of sample means) using Microsoft Excel 2019. An $\alpha = 0.05$ was used to assess statistical significance in all tests.

Results

Material Characterization

The baseline properties of the individual cover materials are summarized in Table 1. The barrier soil had the highest fines content (\sim 90%) followed by the topsoil (\sim 82%) whereas the soil in biochar-amended soil layer had the lowest (\sim 65%). The soil used in biochar-amended soil layer had the highest organic content (4.9%). The organic contents of the soils used in this study

are within the favorable range for methane oxidation as reported by Rachor et al. (2011). The K of the barrier soil layer was 1.3×10^{-7} cm/s. The K of 10% biochar-amended soil was 1.1×10^{-5} cm/s, still satisfying the $K < 10^{-5}$ cm/s RCRA Subtitle D requirement. The water-retention capacity of the barrier soil was slightly higher (\sim 57%), than the biochar-amended soil (55.3%) due to the higher fines content of the barrier soil. Barrier soil had an elevated carbonate content due to its source. The fresh BOF slag had very low carbonate content (\sim 3.8%).

The barrier soil layer was compacted to 87% of its maximum dry density (MDD) resulting in a total porosity of 42% (Table 2). With similar compaction, the dry density of the biochar-amended soil was much lower and its porosity was much higher (51%), likely due to the pelletized form and low density (specific gravity of 0.65) of biochar. The higher bulk and dry densities of BOF slag reflects its elevated iron content and thus specific gravity of 3.34 for comparable porosity. The topsoil layers were also placed with minimal compaction. Porosity has shown to be a critical factor for O_2 intrusion in cover systems, and this in turn affects the methane oxidation rates (Yargicoglu and Reddy 2018; Rachor et al. 2011).

Gas Profiles

Phase I (Preincubation)

During preincubation, a 1,000 ppm CH_4 gas at a flowrate of 5 mL/min or flux rate of 0.2 g CH_4/m^2 -day was introduced into the GDL at the base of each column. The CH_4 concentrations gradually decreased in the flow direction until the quasi-steady state concentrations were obtained after 17 days (Fig. 2) in both profiles. CH_4 was completely removed in the biochar-amended soil and significant CO_2 production was observed. Less CO_2 production was observed in the SC barrier soil. CO_2 generated in the biocharamended soil layer was completely sequestered by the overlying BOF slag layer, achieving zero emissions of CO_2 [Fig. 2(b)]. Oxygen penetration from the overlying air was fairly deep in both columns (70 cm) at the low CH_4 injection rates.

Phase II

On day 18, the gas flow condition was switched to 48.25% CH₄, 50% CO₂, and 1.75% H_2S at 50 g CH_4/m^2 -day. The average quasi-steady state gas concentration profiles of CH₄, CO₂, and O₂ are shown in Figs. 3a (SC) and 3b (BGCC). The CH₄ concentrations were significantly reduced in the biochar-amended soil layer in the BGCC column, achieving a CO₂/CH₄ ratio of 1.6 versus the inlet gas ratio of 1.03 [Fig. 3(b)]. CH₄ and O₂ concentrations were somewhat higher in the barrier soil layer [Fig. 3(a)], suggesting less methanotrophic activity. O₂ concentrations dropped significantly in the biochar-amended soil layer despite its relatively higher porosity (Table 2), suggesting that O₂ was not outgassed by the counter-current flowing LFG but rather consumed by methane-oxidizing bacteria. Numerous other studies have shown that O2 concentrations dropped significantly in zones of CH4 oxidation (Kightley et al. 1995; De Visscher et al. 1999; Rachor et al. 2011; Roncato and Cabral 2012).

Fig. 4 shows the CH_4 , CO_2 , O_2 , and H_2S concentrations at select depths for each column. Significant CH_4 was removed in the BGCC column as shown by reduced concentrations near the top of the biocover (or biologic) layer (35 cm bgs) [Fig. 4(b)]. Only about 10% of the inlet CH_4 reached the headspace [Fig. 4(b)]. CO_2 was completely sequestered in the BOF slag layer, whereas nearly 7% of the LFG CO_2 reached the overlying headspace of the SC system [Fig. 4(c)]. H_2S was completely removed near the inlet of both columns [see Fig. 4(d)], suggesting that the soil itself

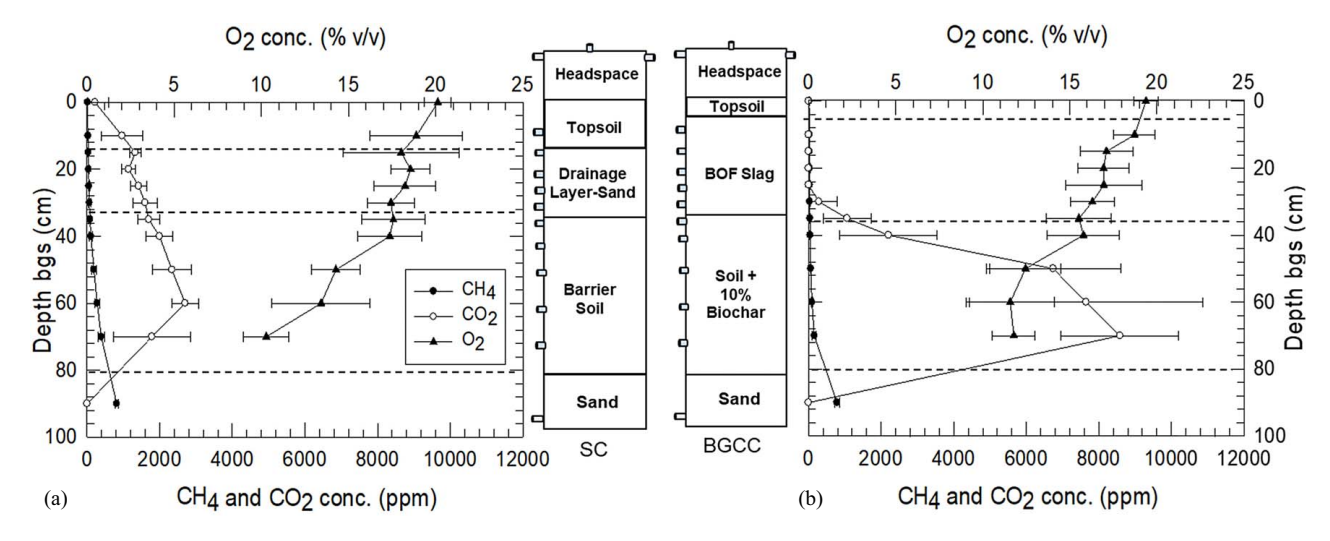


Fig. 2. Quasi-steady state gas concentration profiles during preincubation in: (a) SC; and (b) BGCC.

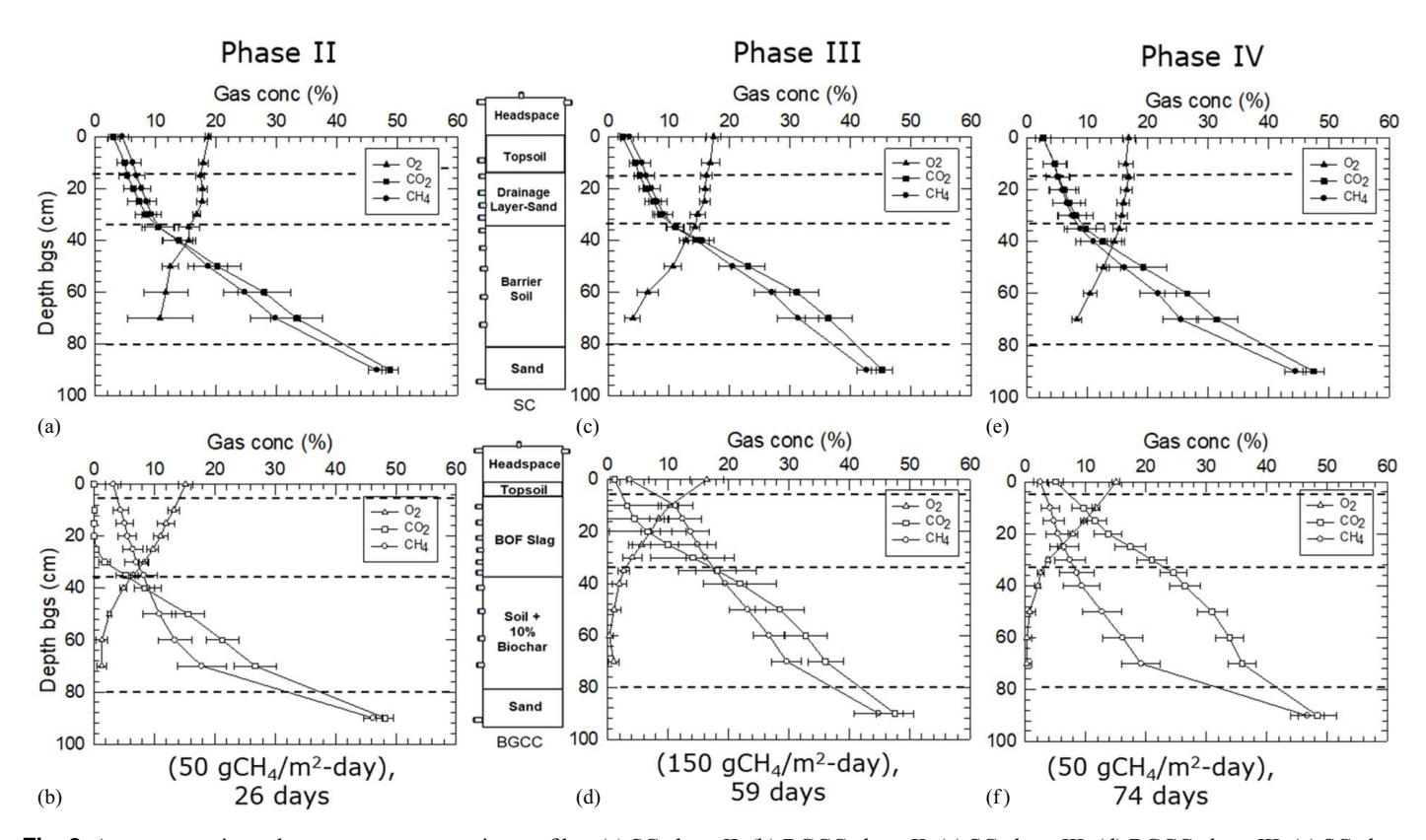


Fig. 3. Average quasi-steady state gas concentration profiles: (a) SC phase II; (b) BGCC phase II; (c) SC phase III; (d) BGCC phase III; (e) SC phase IV; and (f) BGCC phase IV.

had significant H_2S removal potential. Recent studies have shown that biochar possesses significant adsorption potential for gaseous H_2S (Oliveira et al. 2020; Shang et al. 2013) as well as landfill cover soils (Lee et al. 2015; He et al. 2012; Xu et al. 2010), consistent with the observations in this study.

Phase III

In Phase III, the CH_4 inflow rate was tripled to 150 g CH_4/m^2 -day. The CH_4 concentrations at 35 cm bgs and the overlying headspace in both SC and BGCC columns are shown in Fig. 4(b). Corresponding increases in CO_2 concentrations at 35 cm bgs were observed for

both columns; however, the headspace CO_2 concentrations remained undetected for an extended period in the BGCC column [Fig. 4(b)]. The BOF slag experienced complete CO_2 breakthrough after 50 days of Phase III (or 70 days of LFG exposure) [Fig. 4(b)]. Overall, the gas concentration profiles remained similar to those in Phase II except that the O_2 concentration was reduced in the biologic layer of both columns, likely due to outgassing effects (Roncato and Cabral 2012).

A rainfall event was simulated by sprinkling 340 mL (equivalent to a half inch rainfall) of water on the surface of each column 20 days into Phase III (64 days overall). Afterwards, the gas

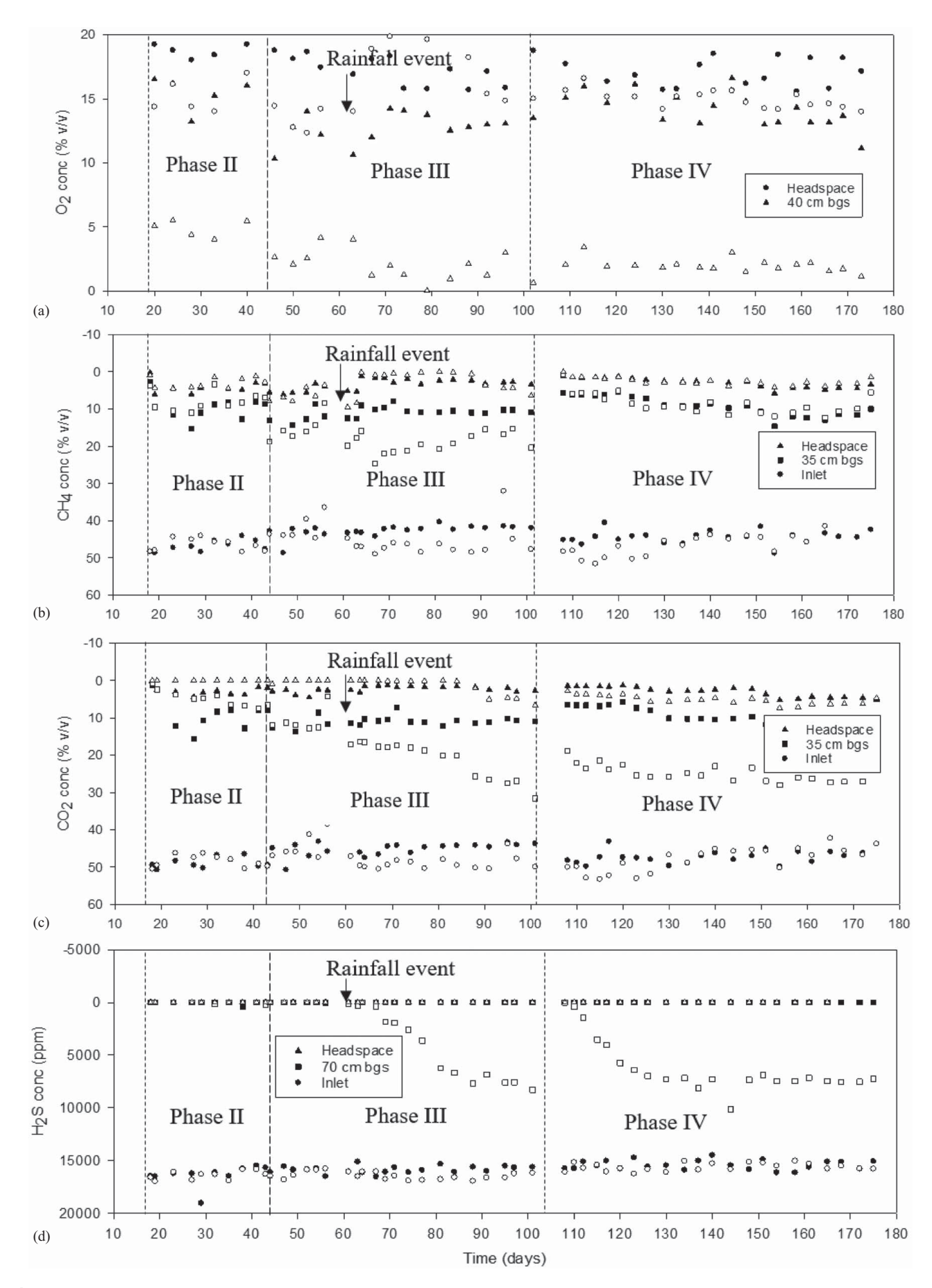


Fig. 4. Gas concentrations as function of time: (a) O_2 ; (b) CH4; (c) CO_2 ; and (d) H_2S . Note: solid symbol is SC and open symbol is BGCC column designations. The *y*-axes in the figures (b), (c), and (d) are inverted to represent the gas flow direction.

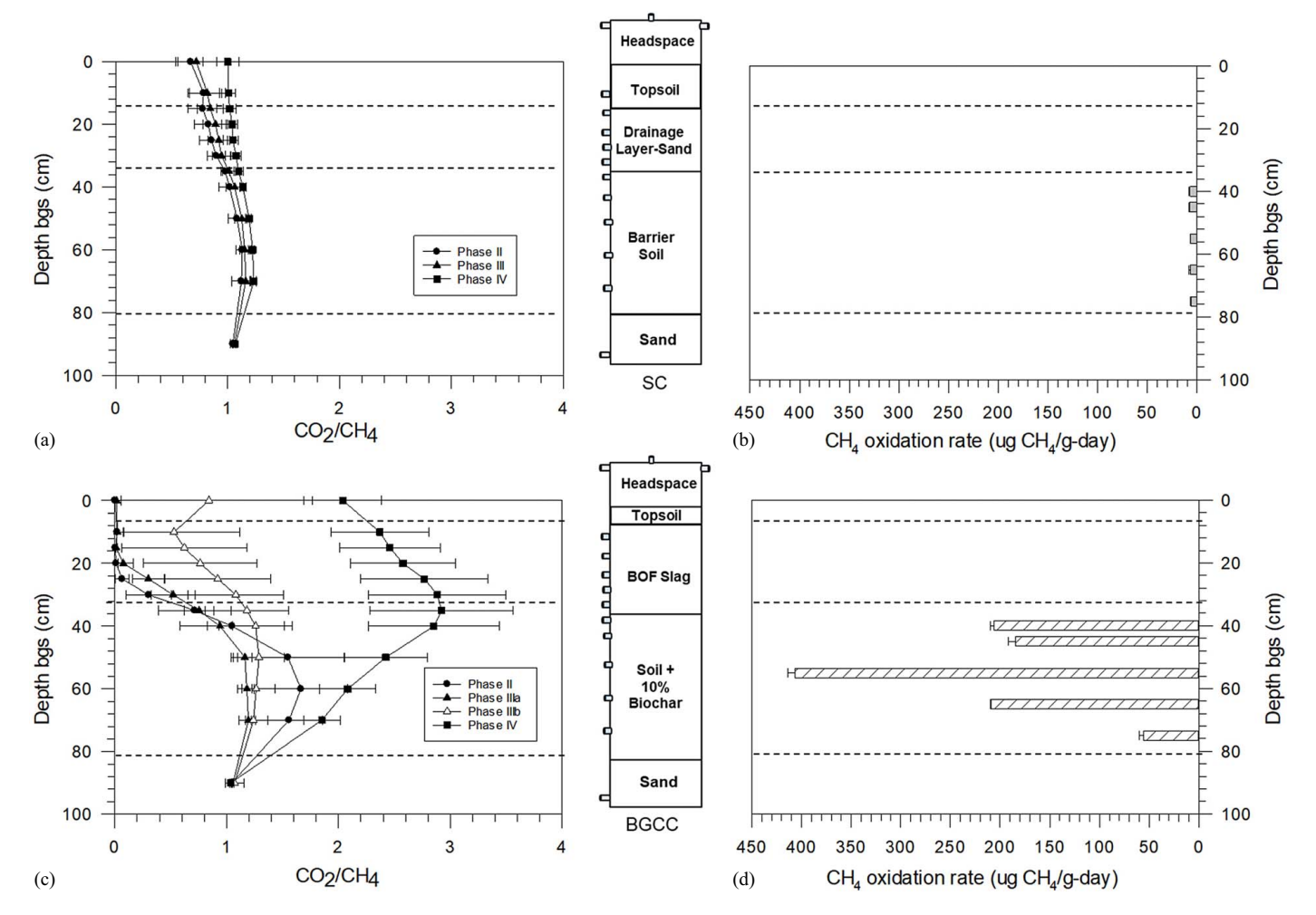


Fig. 5. Average quasi-steady state CO₂/CH₄ and terminal CH₄ oxidation rates with column depth during various operation phases for: (a and b) the SC; and (c and d) BGCC columns.

profiles in the BGCC column changed dramatically. The thin layer of topsoil (~5 cm) over the BOF slag layer became waterlogged, preventing the exchange of gases through that layer. As a result, CH₄ and CO₂ increased in the layer below the topsoil and H₂S also significantly increased in the biologic layer [see 70 cm data in Fig. 4(d)]. Similarly, O₂ penetration into the deeper layers was substantially curtailed following the rainfall event.

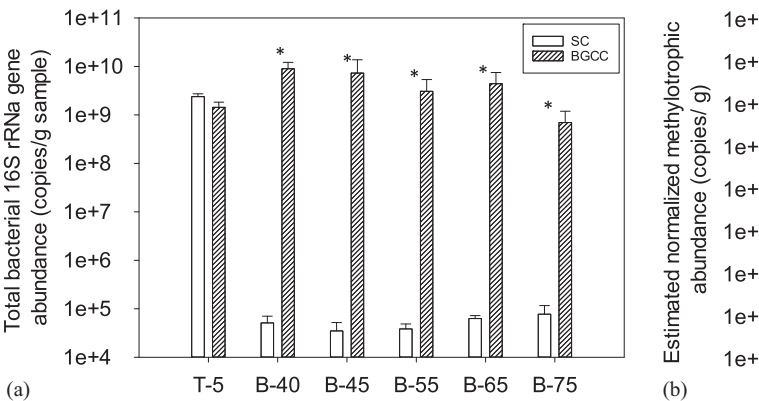
Waterlogging from the rainfall event was not as pronounced in the SC column as the topsoil was relatively thick (15 cm), thus allowing greater water storage. The average vertical gas profiles of CH₄, CO₂, and O₂ in the SC and BGCC columns before and after the rainfall event are shown in Fig. S1. No significant difference was observed in the vertical gas profiles in the SC column before and after the rainfall event [Figs. S1(a and b)]. However, the lower layers (below 60 cm) became nearly anoxic after rainfall [Fig. S1(d)] in the BGCC column. Similarly, CH₄ increased in the upper layers (BOF slag layer), indicating accumulation of gases at the interface of topsoil due to waterlogging. The placement of a thicker topsoil layer over the BOF slag is necessary to preclude such a waterlogging effect. In retrospect, the BOF slag layer should have matched the drainage layer thickness of the SC column.

Phase IV

In Phase IV, the gas flowrate was restored to Phase II levels to investigate if CH₄ oxidation rates would rebound. The gas profiles in

the SC column remained essentially unchanged for Phases II to IV. On the other hand, measurements in the BGCC column demonstrated a substantial reduction in CH₄ and a concomitant increase in CO₂ in the biochar-amended soil layer [Fig. 3(f)], confirming resumption of CH₄ oxidation activity. This shows that lower CH₄ flow rates are needed to prevent less O2 outgassing under waterlogged conditions. In contrast to previous phases, Phase IV showed elevated concentrations of CO2 in the biochar-amended soil layer with only a slight reduction in the BOF slag layer, suggesting the persistence of waterlogging conditions in Phase IV. In addition, the H₂S concentration at the 70 cm depth remained nearly similar to Phase III, further confirming waterlogged conditions. Progressive darkening of the soil layer (Fig. S2), potentially associated with precipitation of sulfur or metal sulfides, was also evident in the BGCC column (Chetri et al. 2020). This process was not observed in the barrier soil layer of the SC column.

The average CO_2/CH_4 ratios were plotted by depth during Phase II, IIIa (before rainfall), IIIb (after rainfall), and IV for both columns (Fig. 5). Deviations from the inlet CO_2/CH_4 ratio (1.03) were used to assess methanotrophic activity. The SC column showed a relatively consistent CO_2/CH_4 profile [Fig. 5(a)], suggesting lower CH_4 oxidation activity. The BGCC column showed significantly higher CO_2/CH_4 ratios (1.66 to 2.96, P < 0.01, ANOVA) mainly during Phases II and IV. During Phase III, the ratio was significantly lower (1.24, P < 0.01, ANOVA) due to waterlogging and reduced O_2 penetration into deeper layers.



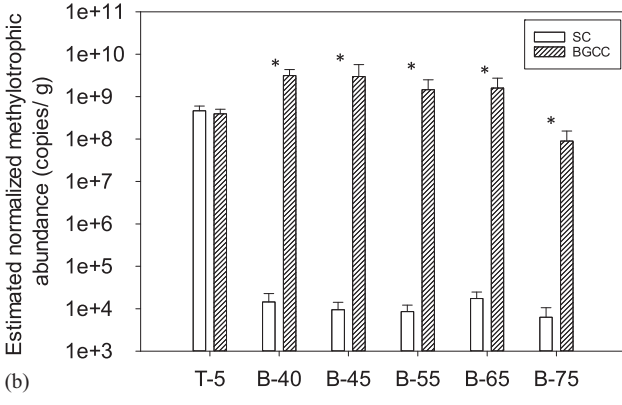


Fig. 6. Absolute abundance of bacterial communities: (a) total 16S rRNA bacterial gene abundance; and (b) estimated normalized methylotrophic bacterial abundance. Note: The "*" sign represents statistically significant differences between the SC and BGCC groups at each depth at a significance level of 95%, ANOVA.

Methane Oxidation Rates

Methane oxidation rates were calculated for the topsoil and biologic soil layers at various depths [Fig. 5(b)]. The average CH₄ oxidation rates of the biochar-amended soils were significantly higher (P=0.01, ANOVA) than that of the barrier soil layer with a peak oxidation rate of 407 µg CH₄/g-day (at 55 cm bgs) [Fig. 5(b)]. This peak value is substantially higher than the oxidation rates previously reported in a similar system and depths (185-210 µg CH₄/g-day at 40-65 cm; Yargicoglu and Reddy 2018). Similar CH₄ oxidation trends with depth (e.g., highest CH₄ oxidation rates at top 20–30 cm of the soil layer) have been previously reported (De Visscher et al. 1999; Yargicoglu and Reddy 2018); in these studies, optimal mixing of CH₄ and O₂ favored the methanotrophic activity. CH₄ oxidation rates at 75 cm bgs were 7.4 to 3.6 times lower than that in the upper strata (40-65 cm bgs), perhaps due to the presence of elevated H₂S. Conversely, the SC system had negligible CH₄ oxidation rates (6-7.5 μg CH₄/g-day) across the barrier soil layer and, thus, a relatively unchanged CO₂/CH₄ ratio [Fig. 5(a)].

Microbial Community Composition

Total measured bacterial 16S rRNA gene abundance was similar (P=0.066, ANOVA) in the topsoil layer of both columns and was in the range of 10⁹ copies/g sample [Fig. 6(a)]. Bacterial gene abundance in the barrier soil layer in the SC column was nearly five orders of magnitude lower than that of the biocharamended soil layer across all depths [Fig. 6(a)]. Consequently, the estimated methylotrophic abundances, calculated by multiplying total bacterial 16S rRNA gene abundances measured by qPCR with relative abundances determined by next-generation amplicon sequencing, revealed significantly lower (P < 0.01, ANOVA) measured absolute abundance of methylotrophs in barrier soil samples in the SC column [Fig. 6(b)]. This is consistent with low CH₄ oxidation rates observed in the barrier soil [Fig. 5(a)]. Possible explanations for the lower microbial activity in the barrier soil could be related to its texture (high clay content), low organic content (Tables 1 and 2), and prior poor CH₄ exposure history at the specific sampling location (Yargicoglu and Reddy 2017b).

Sequencing of 16S rRNA gene amplicons from soil samples from both columns showed diverse microbial communities including methylotrophs, methanotrophs, and heterotrophs. The major phyla detected in both SC and BGCC column samples included

Proteobacteria, Actinobacteria, and Firmicutes [Fig. S3(a)] accounting for 80%–90% of the total sequences, with Proteobacteria being most abundant (35%–60%). Putative aerobic methane-oxidizing bacteria were identified within the Proteobacteria (Alpha- and Gamma-proteobacteria) and Verrucomicrobia (Dedysh and Dunfield 2011; Yargicoglu and Reddy 2017b) [Fig. S3(a)]. The major families detected in the samples included Methylomonaceae, Beijeirinckiaceae, Nicardioidaceae, Burkholderiaceae, Xanthobacteriaceae, and Micromonosporaceae [Fig. S3(b)]. Sequences derived from putative Type I (Methylomonaceae) and Type II (Beijeirinckiaceae) methanotroph lineages were present in these systems.

The methylotrophic relative abundance in the SC column was significantly different from the BGCC column (P = 0.03, ANOVA). The relative abundance of putative methylotrophic bacteria ranged from 10% to 27% in the SC column and from 20% to 51% in the BGCC column [Fig. 7(a)]. From 93% to 99% of putative methylotroph sequences in the SC column samples were putative methanotrophs, except at 75 cm depth (74%). In the BGCC column, 98%-99% of putative methylotrophs were putative methanotrophs, regardless of depth. The relative abundance of putative methanotrophs, as estimated by 16S rRNA gene amplicon sequencing and annotation, was positively correlated with methane oxidation rates in both the SC column ($R^2 = 0.94$, P = 0.006) [Fig. 8(a)] and the BGCC column ($R^2 = 0.88$, P = 0.005) [Fig. 8(b)]. Major methanotrophic groups detected by 16S rRNA gene amplicon sequencing in both column samples included both Type I methanotrophs such as Methylobacter, Methylomicrobium, Crenothrix, Methylocaldum, Methylosarcina, and Type II methanotrophs such as Methylocystis and Methylosinus. Some methanotrophic species that were identified included Methylobacter luteus, Methylocystis hirsute, Methylocaldum gracile, Methylosinus trichosporium, and Methylobacter marinus (Fig. S5). Bacteria from the genus Methylobacter were most prevalent in the barrier soil in the SC column across all depths, accounting for 46%-54% of the total methylotrophs detected. In the BGCC column, bacteria from the genus Methylobacter were only dominant in the bottom 55-75 cm depth (61%-75% of total methylotrophs). Conversely, in the top 35-55 cm with higher CH₄ oxidation [Fig. 5(b)], putative Type II methanotrophs (Methylocystis and Methylosinus) were most abundant and accounted for 49%-54% of putative methylotroph sequences.

The topsoil in the BGCC column was dominated by bacteria from the genus *Methylomicrobium*; these sequences constituted 82% of all putative methylotrophs detected in the topsoil

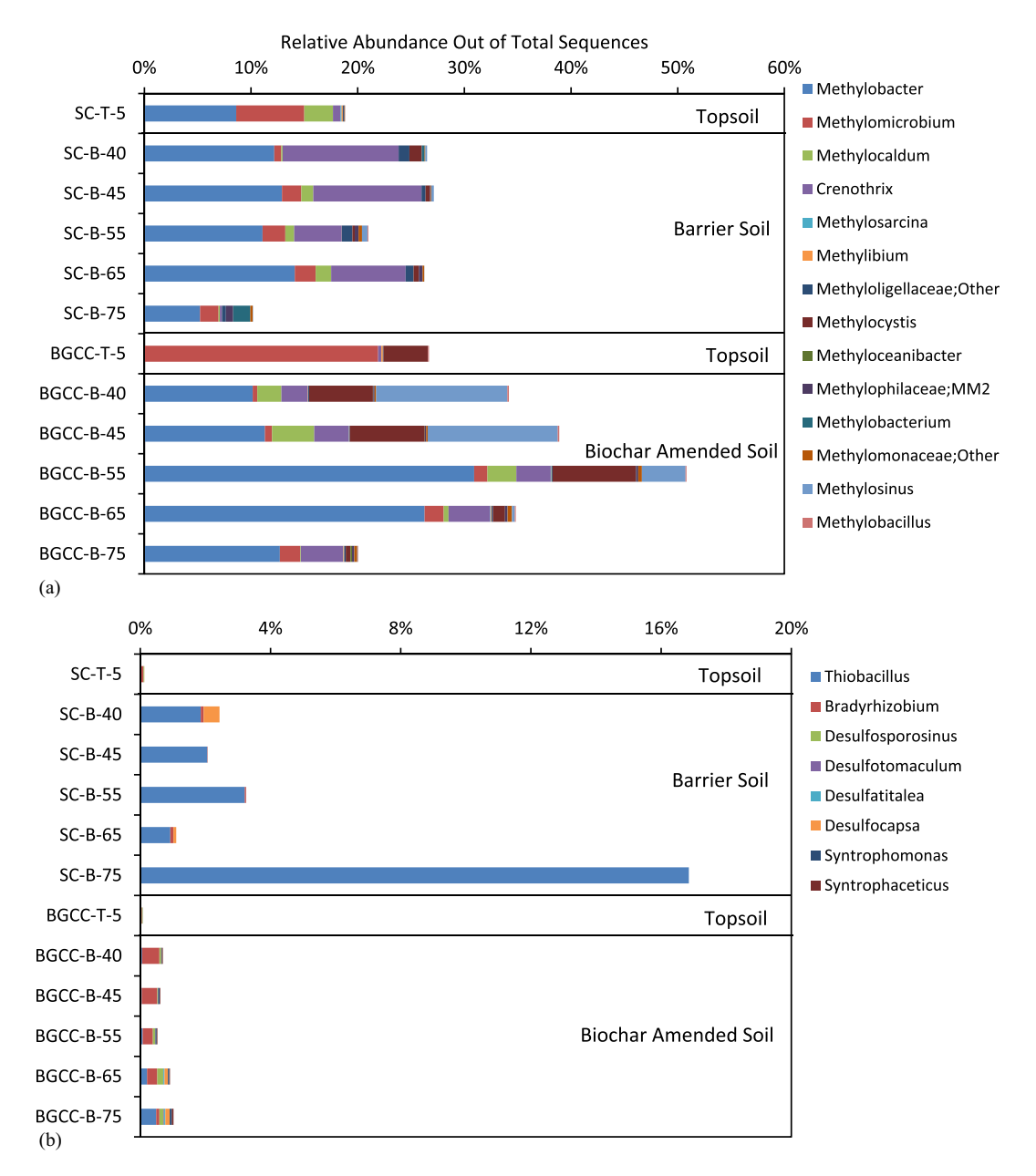


Fig. 7. Relative abundance of (a) methylotrophs; and (b) sulfur oxidizing and reducing bacteria present by column depth.

[Fig. 7(a)]. The dominance of Methylomicrobium over other methanotrophic genera in the topsoil of the BGCC column could be the result of the presence of highly alkaline BOF slag at the interface and the waterlogging event. It is speculated that the geotextile fabric separating BOF slag and topsoil became saturated following the rainfall event and led to an accumulation of calcium ions from BOF slag at the geotextile-slag interface due to wicking effects. Since the topsoil was sampled above the geotextile fabric, it is likely that the soil encountered the alkaline pore fluid through the saturated geotextile. Methylomicrobium are known to be halophilic or alkaliphilic in nature (Kalyuzhnaya et al. 2008; Sorokin et al. 2000). Furthermore, the topsoil sample obtained from the same depth in the SC column had a significantly lower fraction of Methylomicrobium [34% of total methylotrophs; Fig. 7(a)] suggesting that the abundant Methylomicrobium in the BGCC column topsoil were alkaliphilic. Similarly, the barrier soil in the SC column had a significantly higher (P=0.017, ANOVA) relative abundance of methanotrophs from the genus Crenothrix (5%-11% out of total sequences and 21%–41% of total methylotrophs) in comparison to the BGCC column (2.5%–3.9% out of total sequences and 6.3%–19.0% of total methylotrophs). *Crenothrix* have been detected in upland soils and have been associated with atmospheric CH₄ uptake (Knief 2015). The greater abundance of *Crenothrix* in the barrier soil of the SC column correlates well with O₂ concentration profile (Fig. 3).

Effect of H₂S on the Microbial Community Composition

Apart from methylotrophic communities, some known sulfur oxidizing bacterial (SOB) genera, such as *Thiobacillus* (Xia et al. 2015) were detected mainly in the SC column [Fig. 7(b)] ranging from 1% to 17% of the total sequences. This could be due to the higher O₂ availability in the SC column [Figs. 3(a, c, and e)] creating a conducive environment for H₂S oxidation. Two species of *Thiobacillus* were detected, including *T. denitrificans* and *T. thioparus* (Fig. S5). *T. denitrificans* was prevalent at

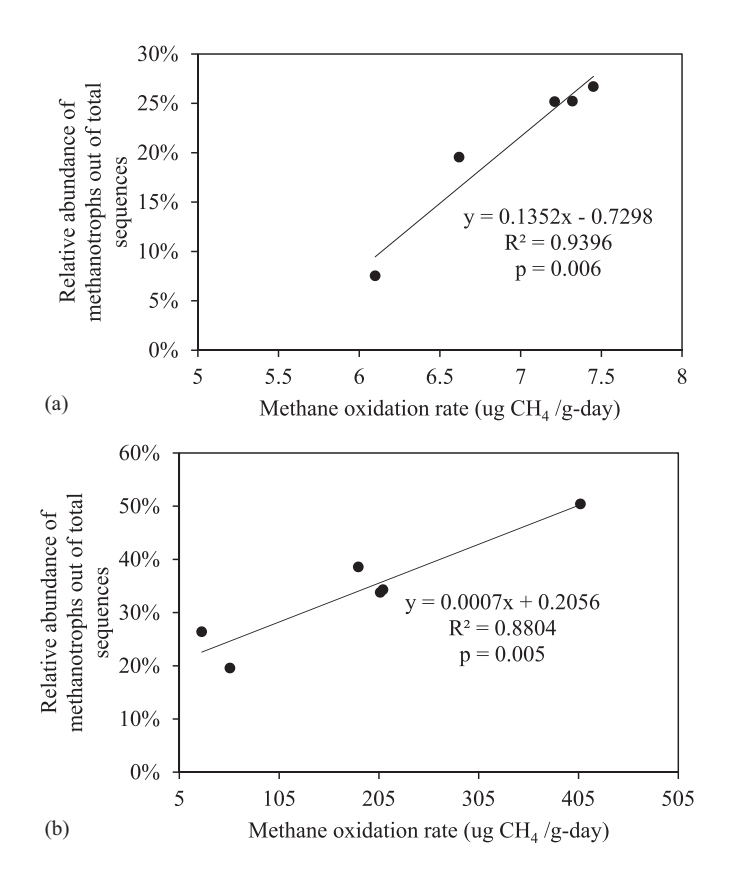


Fig. 8. Relationship between methane oxidation rate and relative abundance of methanotrophic bacteria in bottom soil layer of (a) SC column; and (b) BGCC column. The regression analysis was performed in Excel 2020.

75 cm depth in the SC column; complete removal of H₂S was observed at this depth only in the SC column. Although T. denitrificans are chemoautotrophic facultative anaerobes, they can metabolize H₂S under aerobic conditions (Subletta 1987; Cadenhead and Sublette 1990; Ma et al. 2006). Hence, it is hypothesized that Thiobacillus spp. were responsible for the oxidation and removal of sulfide in the SC column [Fig. 4(d)]. In the BGCC column, the abundance of Thiobacillus was below 1%. The relatively low abundance of Thiobacillus in the biochar-amended soil at 75 cm bgs suggests that H₂S was removed abiotically in the BGCC column. Alternatively, high methanotrophic activity in the biochar-amended soil may have created an O₂ deficiency, thereby limiting the activity of the SOBs. Trace sulfur/sulfate-reducing bacteria (<1%) such as Desulfosporosinus, Desulfotomaculum, Desulfatitalea, and Desulfocapsa (Ramamoorthy et al. 2006; Widdel and Back 2006; Higashioka et al. 2013) were found in the biochar-amended soil, primarily at 65–75 cm bgs. These multiple lines of evidence suggest the reducing conditions dominated the bottommost extremity of the biochar-amended soil.

Terminal Material Properties

After the experiments were terminated, select layers were exhumed and analyzed (Table 4). The initial MC of the topsoil in both the columns was 15%. The final MC in the topsoil of the BGCC column was higher (23.3%) than that of SC column (~19%), suggesting prolonged waterlogging of the topsoil. Other topsoil parameters such as OC, pH, and carbonate content in the SC column did not vary significantly from the initial conditions (Table 4) nor did the MC of the barrier soil and drainage sand.

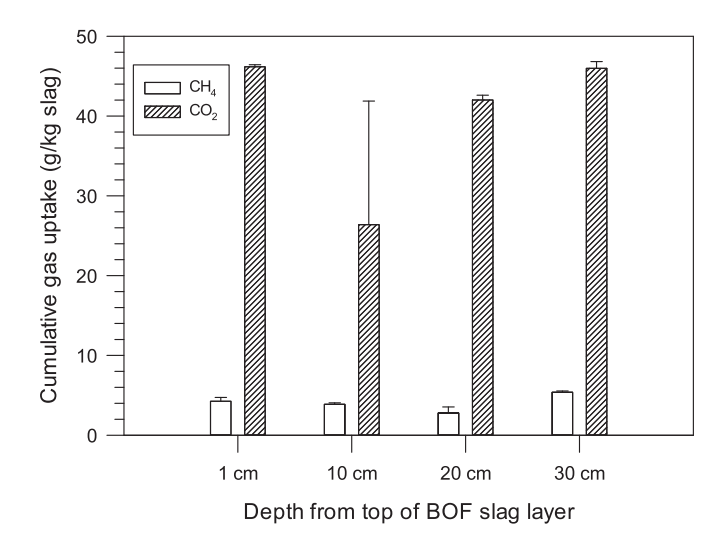


Fig. 9. Residual CH₄ and CO₂ removal capacity of the exhumed BOF slag.

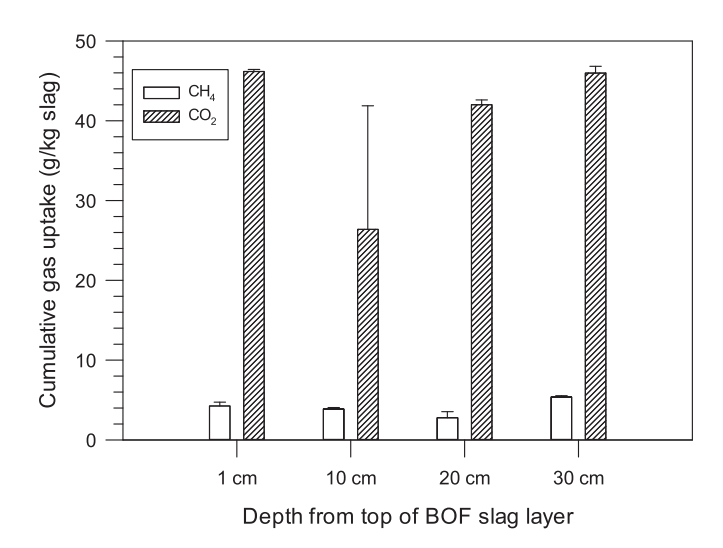


Fig. 10. Solid mark represents the carbon and open mark represents the sulfur content of exhumed samples.

A slight increase in MC was observed in both the BOF slag and biochar-amended soil layers of the BGCC column, which could be attributed to the downward flow of water or potential H₂O production during carbonation and CH₄ oxidation reactions. The final LOI of the GDL sand was slightly higher (0.5%–0.6%) than its original value (0.3%). This could be a result of the sulfur precipitation from H₂S, as darkening of the GDL sand was more prominent in BGCC column than SC (Fig. S2). The pH of the BOF slag decreased from 12.4 to between 11.31 and 11.74, likely due to carbonation reactions consuming residual lime (CaO) and portlandite [Ca(OH)₂] (Huijgen and Comans 2006; van Zomeren et al. 2011; Chetri et al. 2019). Carbonation of BOF slag was further confirmed by the significant increase in its calcium carbonate content from an initial 3.8% to 15%-19%. The 15.2% (or 0.15 g CaCO₃) increase corresponds to CO₂ removal capacity of 67 g CO₂/kg BOF slag or lower than the CO₂ removal capacity previously reported for this slag (Chetri et al. 2020). Batch tests were thus performed on the carbonated BOF slag obtained from various depths of the BOF slag layer to quantify its residual carbonation capacity (Fig. 9). The residual CO₂ removal capacity ranged from 26 to 46 g CO₂/kg

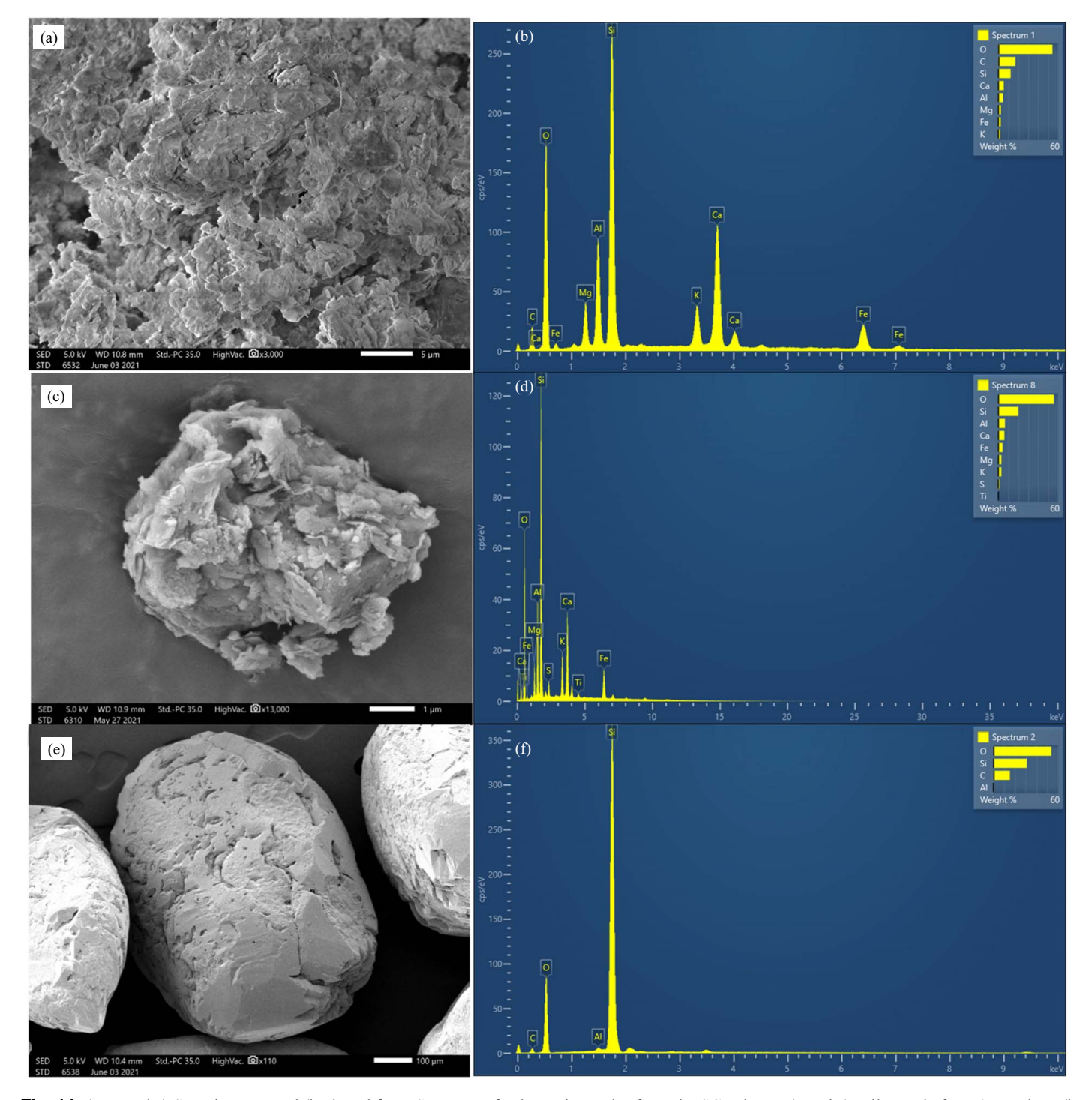


Fig. 11. (a, c, and e) SEM images and (b, d, and f) EDS spectra of exhumed samples from the SC column: (a and c) soil sample from 35 cm bgs; (b and d) soil sample from 75 cm bgs; and (c and e) sand sample from GDL.

slag, exhibiting considerable CO_2 removal potential even after a breakthrough in the column reactor. The temperature of the soil layers as monitored by the sensors did not show any significant change during the entire column operation period (Fig. S8) and were in equilibrium with the room temperature. Thus, microbial activity or carbonation of the slag did not increase the temperature, despite mineral carbonation and microbial CH_4 oxidation reactions being slightly exothermic (Mazzotti et al. 2005; Sadasivam and Reddy 2014).

The total carbon and sulfur content in the barrier soil layer in the SC column and biochar-amended soil and BOF slag layers in the BGCC column are shown in Fig. 10. The total carbon content is

similar to the initial OC/LOI in the SC and the BGCC column, however, a spike in sulfur content (\sim 0.7%) was observed in both the columns at 75 cm bgs where most of the H₂S was absorbed. The sulfur content of the BOF slag layer remained much lower than the biochar-amended soil layer at a 75 cm depth, suggesting H₂S did not reach the BOF slag layer during column operation.

These observations show that the waterlogging of the BGCC column affected gas flow and reduced the CO_2 removal capacity of the BOF slag. This has significant implications in the design life of the BOF slag for field applications. For example, assuming a landfill cover of an area of 1 hectare (10^4 m^2) with a 30 cm-thick

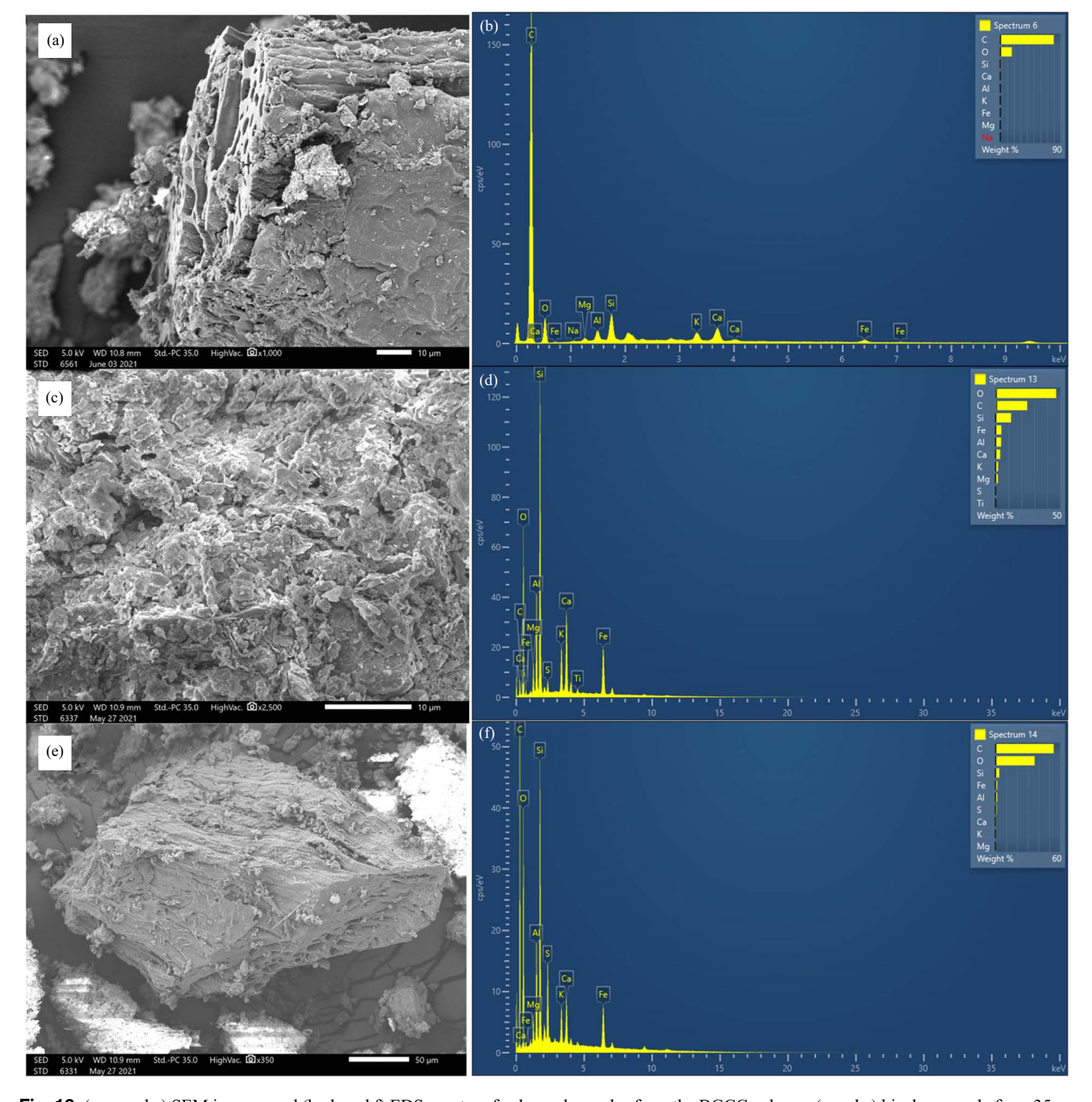


Fig. 12. (a, c, and e) SEM images and (b, d, and f) EDS spectra of exhumed samples from the BGCC column: (a and c) biochar sample from 35 cm bgs; (b and d) soil sample from 75 cm bgs; and (c and e) biochar sample from 75 cm bgs.

BOF slag cover with dry density 1,700 kg/m³ and CO₂ influx of 50 g CO₂/m²-day, the estimated design life of the BOF slag will be:

- 1.9 years for the CO₂ removal capacity of 67 g CO₂/kg BOF slag (as obtained in this study);
- 3.4 years for the CO₂ removal capacity of 120 g CO₂/kg BOF slag [as obtained in Chetri et al. (2020) for slag as-is]; and
- 8.4 years for the CO₂ removal capacity of 300 g CO₂/kg BOF slag [as obtained in Chetri et al. (2020) for fine slag], which is almost one-third of the postclosure period.

This shows that a poorly designed BGCC cover system can significantly impact the design life of BOF slag to scrub CO_2 from

fugitive LFGs. Since the combined residual lime/portlandite content of fresh BOF slag is in the order of 10% to 15% (6.3% in this study), there is major motivation to leverage the $\rm CO_2$ sequestration capacity of BOF slag for at least the entire postclosure period (30 years).

Mineralogical Changes in LFG Exposed Samples

The final mineralogical composition of the barrier soil, biocharamended soil, and BOF slag-based on QXRD analysis is summarized in Table 5. The calcite and dolomite contents of the landfill

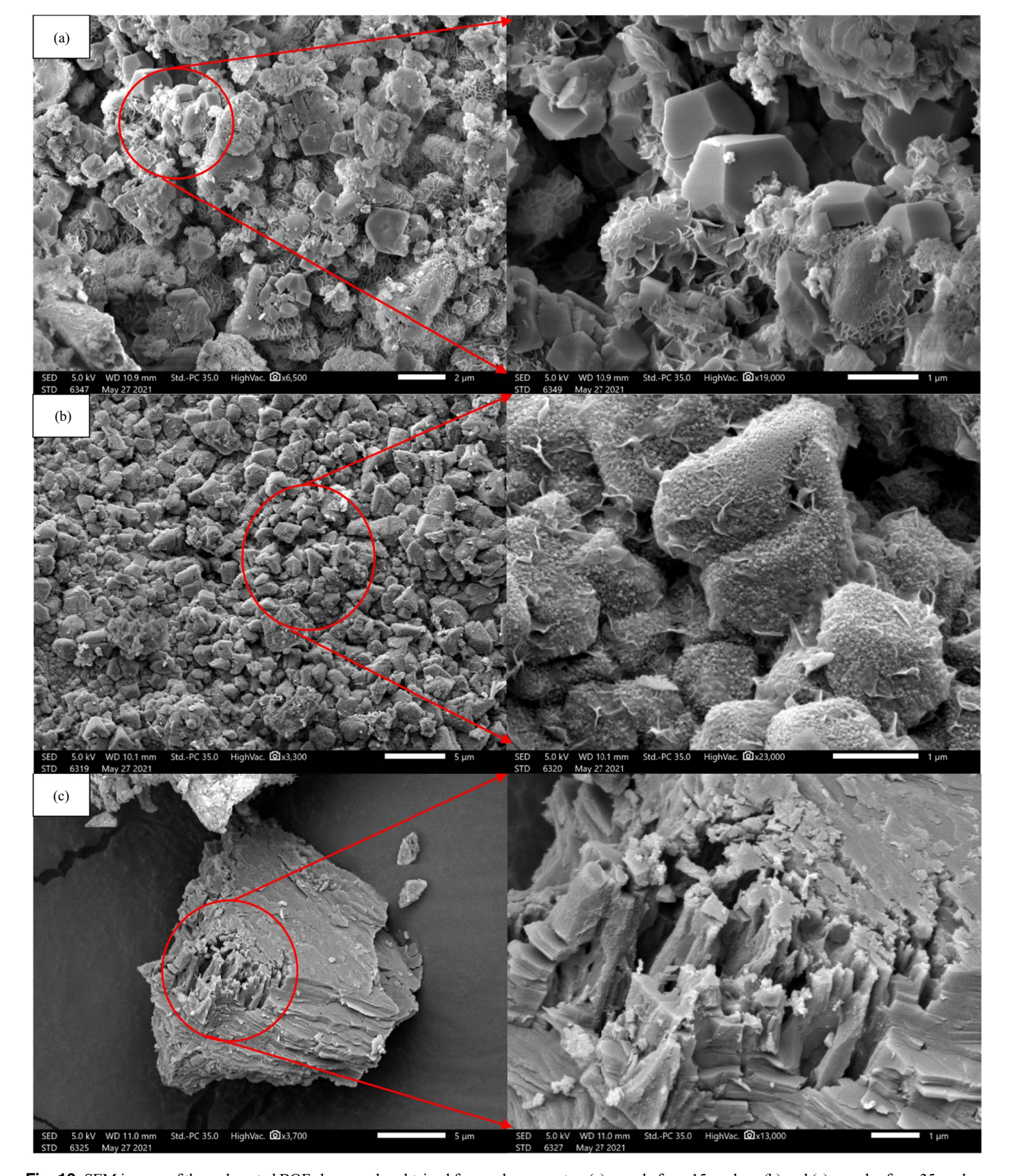


Fig. 13. SEM images of the carbonated BOF slag samples obtained from column reactor: (a) sample from 15 cm bgs; (b) and (c) samples from 35 cm bgs.

cover soils are consistent with the high initial carbonate content (Table 1). The calcite content of the exhumed BOF slag was significantly higher (13.6%) than its initial carbonate content. Portlandite $[Ca(OH)_2]$ was not detected in the carbonated BOF slag, suggesting

it reacted completely during LFG exposure. Assuming the BOF slag had initially 4.67% Ca(OH)₂ and it reacted completely with CO₂, the CO₂ removal corresponds to 27 g CO₂/kg slag. Similarly, lime (CaO) reduction from 1.76% to 1.2% correspond to 3.9 g

 $\mathrm{CO_2/kg}$ slag. However, the increase in calcite content (13.17%) corresponds to 58 g $\mathrm{CO_2/kg}$ slag. This suggests minerals other than lime and portlandite (such as larnite and brownmillerite) may have sufficient alkalinity and buffer capacity to drive long-term $\mathrm{CO_2}$ adsorption.

Morphological Changes in LFG Exposed Samples

SEM micrographs of the barrier soil in the SC system did not show any crystalline fractions resembling carbonates [Figs. 11(a and c)]. EDS spectra showed the presence of iron, which means soil inherently had exposed iron surfaces and thus precipitation of sulfur from reaction with H₂S may have been the mechanism for H₂S removal. In addition, sulfur was detected in samples at 75 cm bgs [Fig. 11(c) and Table S1] further affirming precipitation of sulfur or formation of sulfides near the inlet. The GDL sand in the SC column was also analyzed with SEM/EDS to investigate if H₂S was adsorbed but no sulfur was detected [Fig. 11(e)].

Fig. 12 shows the SEM/EDS results for the biochar-amended soil in the BGCC column from 35 to 75 cm bgs. Biochar particles have highly porous structures with high internal porosity, which is reflected in the SEM micrographs [Figs. 12(a and e)]. Biochar had high carbon content as shown in EDS spectra since it is derived from biomass (pinewood). In addition, biochar also showed presence of iron, which enables adsorption of H_2S . Sulfur was detected in significant quantities in the biochar at 75 cm bgs [Fig. 12(e) and Table S1], confirming H_2S removal. The soil particles from the same biochar-amended soil at 75 cm bgs also showed the presence of sulfur [Fig. 12(c) and Table S1].

Fig. 13 shows SEM images of the carbonated BOF slag from the top 10 cm (15 cm bgs) and bottom 30 cm (35 cm bgs) of its layer. At the top, rhombohedral calcite crystals precipitated on the slag surface [Fig. 13(a)], but an overall porous structure persisted, suggesting the slag surface was not completely plugged with precipitates. At the bottom of the layer, more densely packed carbonate crystals were evident [Figs. 13(b and c)] due to the richer CO₂ conditions. The slag particle in Fig. 13(c) showed large, densely packed calcite crystals, but the porosity was retained suggesting that carbonation and potential pore clogging may not be a uniform process in BOF slag (Yilmaz et al. 2013, 2010).

To further investigate if the carbonation of BOF slag affected its K, a parallel BOF slag sample was exposed to a continuous flow of 50% CH₄ and 50% CO₂ as described by Chetri et al. (2020). The BOF slag sample solidified from carbonation as shown in Fig. S7, and the corresponding K was 3.1×10^{-3} cm/s, that is, the same order of magnitude as the fresh BOF slag (Table 1). As such, the carbonation of BOF slag under LFG conditions does not necessarily reduce the K value, perhaps due to nonuniform distribution of residual lime (and thus carbonate precipitation) as was observed in SEM micrographs (Fig. 13).

Conclusions

The potential of a newly proposed biogeochemical landfill cover system to remove CH_4 , CO_2 , and H_2S simultaneously was compared with a conventional SC through column incubation experiments. The BGCC comprised 10% (w/w) biochar-amended soil overlain by BOF slag and topsoil layers, whereas the conventional SC included a compacted barrier soil layer overlain by drainage and topsoil layers. The following observations can be made from this study:

- 1. Both cover systems showed significant H₂S removal, resulting in complete removal in the bottommost part of the bottom biologic layer (70–80 cm bgs).
- 2. A potentially inhibitory effect of H₂S was observed on the CH₄ oxidation rates as biochar-amended soil showed nearly 3.6–7.3 times less CH₄ oxidation rates at 75 cm depth than the upper horizons of the biochar-amended soil layer. This effect was more prominent in the barrier soil in the SC column, which showed a greater abundance of sulfur oxidizing bacteria from the genus *Thiobacillus* (maximum relative abundance of 16%).
- 3. Methane oxidation rates in the biochar-amended soil layer in BGCC column were significantly higher (with maximum of $407 \mu g \text{ CH}_4/\text{g-day}$) than the barrier soil layer in SC (maximum of $8 \mu g \text{ CH}_4/\text{g-day}$).
- 4. The BGCC cover showed significant potential to mitigate CH₄, CO₂, and H₂S. Greater than 90% removal of CH₄ and 100% removal of H₂S occurred mainly under low CH₄ flow conditions (50 g CH₄/m²-day). Zero emissions of CO₂ were achieved for a limited period (corresponding to ~2 years in the field setting assuming 50 g CO₂/m²-day flux) due to waterlogging problems. For the same gas injection conditions, the SC cover showed 100% removal of H₂S but emitted CH₄ and CO₂ in considerable amounts.
- 5. BOF slag underwent significant carbonation during column incubation resulting in maximum carbonate content of 0.19 g CaCO₃, which corresponds to CO₂ removal of 67 g CO₂/kg BOF slag. QXRD analysis showed exhaustion of portlandite [Ca(OH)₂] but persistence of lime (CaO). Waterlogging of the thin topsoil layer limited the carbonation potential of the BOF slag, by approximately 40 g CO₂/kg BOF. This design flaw will be corrected in a future study.
- 6. While BOF slag is susceptible to pore clogging with precipitation of carbonate crystals, its *K* and gas flow were not reduced significantly.

Overall, the proposed biogeochemical cover shows excellent promise to mitigate CH_4 , CO_2 , and H_2S under simulated landfill conditions and thus offers a sustainable alternative to conventional SC systems.

Data Availability Statement

The raw sequence data (FASTQ files) for this project were deposited in the National Center for Biotechnology Information (NCBI) Sequence Read Archive (SRA), under the BioProject identified PRJNA760791. All other data generated during the study appear in this article.

Acknowledgments

This research is a part of comprehensive project titled "Innovative Biochar-Slag-Soil Cover System for Zero Emissions at Landfills" funded by the National Science Foundation (CMMI# 1724773), which is gratefully acknowledged. Any opinions, findings, conclusions, and recommendations expressed in this material are those of the authors and do not necessarily reflect the views of the NSF. The authors would like to thank Phoenix Services LLC for supplying BOF slag for this study. The authors are grateful to Genomic Research Core and Electron Microscopy Core, Research Resources Center, University of Illinois at Chicago for microbial analysis. Pittsburgh Mineral & Environmental Technology, Inc. (PMET Lab Services) conducted the QXRD and carbon/sulfur analysis of the samples.

Supplemental Materials

Table S1 and Figs. S1–S8 can be found online in the ASCE Library (www.ascelibrary.org).

References

- ASTM. 2014. Standard test methods for specific gravity of soil solids by water pycnometer. ASTM D854-14. West Conshohocken, PA: ASTM.
- ASTM. 2016. Standard test methods for measurement of hydraulic conductivity of saturated porous materials using a flexible wall permeameter. ASTM D5084-16a. West Conshohocken, PA: ASTM.
- ASTM. 2017a. Standard test methods for particle-size distribution (gradation) of soils using sieve analysis. ASTM D6913/D6913M-17. West Conshohocken, PA: ASTM.
- ASTM. 2017b. Standard test method for saturated density, moistureholding capacity, and porosity of saturated peat materials. ASTM D2980-17e1. West Conshohocken, PA: ASTM.
- ASTM. 2019a. Standard test methods for pH of soils. ASTM D4972-19. West Conshohocken, PA: ASTM.
- ASTM. 2019b. Standard test method for permeability of granular soils (constant head). ASTM D2434-19. West Conshohocken, PA: ASTM.
- ASTM. 2019c. Standard test methods for pH of soils. ASTM D4972-19. West Conshohocken, PA: ASTM.
- ASTM. 2020. Standard test methods for determining the water (moisture) content, ash content, and organic material of peat and other organic soils. ASTM D2974-20e1. West Conshohocken, PA: ASTM.
- ASTM. 2021a. Standard test methods for laboratory compaction characteristics of soil using standard effort (12,400 ft-lbf/ft³ (600 kN-m/m³)). ASTM D698-12. West Conshohocken, PA: ASTM.
- ASTM. 2021b. Standard test method for rapid determination of carbonate content of soils. ASTM D4373-21. West Conshohocken, PA: ASTM.
- Bolyen, E., et al. 2019. "Reproducible, interactive, scalable and extensible microbiome data science using QIIME 2." *Nat. Biotechnol.* 37 (8): 852–857. https://doi.org/10.1038/s41587-019-0209-9.
- Bogner, J. E., K. A. Spokas, and J. P. Chanton. 2011. "Seasonal greenhouse gas emissions (methane, carbon dioxide, nitrous oxide) from engineered landfills: Daily, intermediate, and final California cover soils." *J. Environ. Qual.* 40 (3): 1010–1020. https://doi.org/10.2134/jeq2010 .0407.
- Cadenhead, P., and K. L. Sublette. 1990. "Oxidation of hydrogen sulfide by Thiobacilli." *Biotechnol. Bioeng.* 35 (11): 1150–1154. https://doi.org/10.1002/bit.260351111.
- Chetri, J. K., and K. R. Reddy. 2021. "Advancements in municipal solid waste landfill cover system: A review." *J. Indian Inst. Sci.* 101: 557–588. https://doi.org/10.1007/s41745-021-00229-1.
- Chetri, J. K., K. R. Reddy, and D. G. Grubb. 2019. "Innovative biogeochemical cover to mitigate landfill gas emissions: Investigation of controlling parameters based on batch and column experiments." *Environ. Processes* 6 (4): 935–949. https://doi.org/10.1007/s40710-019-00390-x.
- Chetri, J. K., K. R. Reddy, and D. G. Grubb. 2020. "Carbon-dioxide and hydrogen-sulfide removal from simulated landfill gas using steel slag." *J. Environ. Eng.* 146 (12): 04020139. https://doi.org/10.1061/(ASCE)EE.1943-7870.0001826.
- Chetri, J. K., K. R. Reddy, and S. J. Green. 2022a. "Methane oxidation and microbial community dynamics in activated biochar-amended landfill soil cover." *J. Environ. Eng.* 148 (4): 04022009. https://doi.org/10 .1061/(ASCE)EE.1943-7870.0001984.
- Chetri, J. K., K. R. Reddy, and D. G. Grubb. 2022b. "Investigation of different biogeochemical cover configurations for mitigation of landfill gas emissions: Laboratory column experiments." Acta Geotech. 1–18.
- Dedysh, S. N., and P. F. Dunfield. 2011. "Facultative and obligate methanotrophs: How to identify and differentiate them." *Methods Enzymol.* 495: 31–44. https://doi.org/10.1016/B978-0-12-386905-0.00003-6.
- De Visscher, A., D. Thomas, P. Boeckx, and O. Van Cleemput. 1999. "Methane oxidation in simulated landfill cover soil environments." *Environ. Sci. Technol.* 33 (11): 1854–1859. https://doi.org/10.1021/es9900961.

- Ding, Y., J. Xiong, B. Zhou, J. Wei, A. Qian, H. Zhang, W. Zhu, and J. Zhu. 2019. "Odor removal by and microbial community in the enhanced landfill cover materials containing biochar-added sludge compost under different operating parameters." Waste Manage. (Oxford) 87: 679–690. https://doi.org/10.1016/j.wasman.2019.03.009.
- He, R., F.-F. Xia, Y. Bai, J. Wang, and D.-S. Shen. 2012. "Mechanism of H₂S removal during landfill stabilization in waste biocover soil, an alterative landfill cover." *J. Hazard. Mater.* 217–218: 67–75. https://doi .org/10.1016/j.jhazmat.2012.02.061.
- Higashioka, Y., H. Kojima, M. Watanabe, and M. Fukui. 2013. "Desulfatitalea tepidiphila gen. nov., sp. nov., a sulfate-reducing bacterium isolated from tidal flat sediment." *Int. J. Syst. Evol. Microbiol.* 63 (Pt_2): 761–765. https://doi.org/10.1099/ijs.0.043356-0.
- Huijgen, W. J., and R. N. Comans. 2006. "Carbonation of steel slag for CO₂ sequestration: Leaching of products and reaction mechanisms." *Environ. Sci. Technol.* 40 (8): 2790–2796. https://doi.org/10.1021/es052534b.
- Kalyuzhnaya, M. G., V. Khmelenina, B. Eshinimaev, D. Sorokin, H. Fuse, M. Lidstrom, and Y. Trotsenko. 2008. "Classification of halo(alkali) philic and halo(alkali)tolerant methanotrophs provisionally assigned to the genera Methylomicrobium and Methylobacter and emended description of the genus Methylomicrobium." *Int. J. Syst. Evol. Microbiol.* 58 (3): 591–596. https://doi.org/10.1099/ijs.0.65317-0.
- Kightley, D., D. B. Nedwell, and M. Cooper. 1995. "Capacity for methane oxidation in landfill cover soils measured in laboratory-scale soil microcosms." *Appl. Environ. Microbiol.* 61 (2): 592–601. https://doi.org/10 .1128/aem.61.2.592-601.1995.
- Knief, C. 2015. "Diversity and habitat preferences of cultivated and uncultivated aerobic methanotrophic bacteria evaluated based on pmoA as molecular marker." Front. Microbiol. 6: 1346. https://doi.org/10.3389/fmicb.2015.01346.
- Lee, E.-H., K.-E. Moon, T.-G. Kim, S.-D. Lee, and K.-S. Cho. 2015. "Inhibitory effects of sulfur compounds on methane oxidation by a methane-oxidizing consortium." *J. Biosci. Bioeng.* 120 (6): 670–676. https://doi.org/10.1016/j.jbiosc.2015.04.006.
- Ma, Y.-L., B.-L. Yang, and J.-L. Zhao. 2006. "Removal of H₂S by *Thiobacillus* denitrificans immobilized on different matrices." *Bioresour. Technol.* 97 (16): 2041–2046. https://doi.org/10.1016/j.biortech.2005.09.023.
- Mazzotti, M., J. C. Abanades, R. Allam, K. S. Lackner, F. Meunier, E. Rubin, J. C. Sanchez, K. Yogo, and R. Zevenhoven. 2005. "Mineral carbonation and industrial uses of carbon dioxide." In *IPCC special report on carbon dioxide capture and storage*, edited by B. Eliasson and R. T. M. Sutamihardja, 319–338. Cambridge University Press.
- Nadkarni, M. A., F. E. Martin, N. A. Jacques, and N. Hunter. 2002. "Determination of bacterial load by real-time PCR using a broad-range (universal) probe and primers set." *Microbiology* 148 (1): 257–266. https://doi.org/10.1099/00221287-148-1-257.
- Oliveira, F. R., K. C. Surendra, D. P. Jaisi, H. Lu, G. Unal-Tosun, S. Sung, and S. K. Khanal. 2020. "Alleviating sulfide toxicity using biochar during anaerobic treatment of sulfate-laden wastewater." *Bioresour. Technol.* 301: 122711. https://doi.org/10.1016/j.biortech.2019.122711.
- Rachor, I., J. Gebert, A. Gröngröft, and E. M. Pfeiffer. 2011. "Assessment of the methane oxidation capacity of compacted soils intended for use as landfill cover materials." Waste Manage. 31 (5): 833–842. http://doi.org/ 10.1016/j.wasman.2010.10.006.
- Ramamoorthy, S., H. Sass, H. Langner, P. Schumann, R. M. Kroppenstedt, S. Spring, J. Overmann, and R. F. Rosenzweig. 2006. "Desulfosporosinus lacus sp. nov., a sulfate-reducing bacterium isolated from pristine freshwater lake sediments." *Int. J. Syst. Evol. Microbiol.* 56 (12): 2729–2736. https://doi.org/10.1099/ijs.0.63610-0.
- Reddy, K. R., J. K. Chetri, G. Kumar, and D. G. Grubb. 2019. "Effect of basic oxygen furnace slag type on carbon dioxide sequestration from landfill gas emissions." *Waste Manage*. 85: 425–436. https://doi.org /10.1016/j.wasman.2019.01.013.
- Reddy, K. R., E. N. Yargicoglu, and J. K. Chetri. 2021. "Effects of biochar on methane oxidation and properties of landfill cover soil: Long-term column incubation tests." *J. Environ. Eng.* 147 (1): 04020144. https://doi.org/10.1061/(ASCE)EE.1943-7870.0001829.

- Roncato, C. D. L., and A. R. Cabral. 2012. "Evaluation of methane oxidation efficiency of two biocovers: Field and laboratory results." J. Environ. Eng. 138 (2): 164–173. https://doi.org/10.1061/(ASCE)EE.1943-7870.0000475.
- Sadasivam, B. Y., and K. R. Reddy. 2014. "Landfill methane oxidation in soil and bio-based cover systems: A review." Rev. Environ. Sci. Biotechnol. 13 (1): 79–107. https://doi.org/10.1007/s11157-013-9325-z.
- Sadasivam, B. Y., and K. R. Reddy. 2015. "Adsorption and transport of methane in biochars derived from waste wood." Waste Manage. (Oxford) 43: 218–229. https://doi.org/10.1016/j.wasman.2015.04.025.
- Scheutz, C., and P. Kjeldsen. 2005. "Biodegradation of trace gases in simulated landfill soil." J. Air Waste Manage. Assoc. 55 (7): 878–885. https://doi.org/10.1080/10473289.2005.10464693.
- Scheutz, C., G. B. Pedersen, G. Costa, and P. Kjeldsen. 2009. "Biodegradation of methane and halocarbons in simulated landfill biocover systems containing compost materials." *J. Environ. Qual.* 38 (4): 1363–1371. https://doi.org/10.2134/jeq2008.0170.
- Shang, G., G. Shen, L. Liu, Q. Chen, and Z. Xu. 2013. "Kinetics and mechanisms of hydrogen sulfide adsorption by biochars." *Bioresour. Technol.* 133: 495–499. https://doi.org/10.1016/j.biortech.2013.01.114.
- Sorokin, D. Y., B. E. Jones, and J. G. Kuenen. 2000. "An obligate methylotrophic, methane-oxidizing Methylomicrobium species from a highly alkaline environment." *Extremophiles* 4 (3): 145–155. https://doi.org/10.1007/s007920070029.
- Subletta, K. L. 1987. "Aerobic oxidation of hydrogen sulfide by Thiobacillus denitrificans." *Biotechnol. Bioeng.* 29 (6): 690–695. https://doi.org/10.1002/bit.260290605.
- USEPA. 2021. Basic information about Landfill Gas. Landfill Methane Outreach Program (LMOP). Washington, DC: USEPA.
- van Zomeren, A., S. R. Van der Laan, H. B. Kobesen, W. J. Huijgen, and R. N. Comans. 2011. "Changes in mineralogical and leaching properties of converter steel slag resulting from accelerated carbonation at low CO₂ pressure." Waste Manage. 31 (11): 2236–2244. https://doi .org/10.1016/j.wasman.2011.05.022.
- Widdel, F., and F. Back. 2006. "The genus Desulfotomaculum." *Prokaryotes* 4: 787–794. https://doi.org/10.1007/0-387-30744-3_25.

- Xia, F., X. Liu, Y. Kang, R. He, and Z. Wu. 2015. "Elimination of sulphur odours at landfills by bioconversion and the corona discharge plasma technique." *Environ. Technol.* 36 (23): 2959–2966. https://doi.org/10.1080/09593330.2014.957244.
- Xie, T., K. R. Reddy, C. Wang, E. Yargicoglu, and K. Spokas. 2015. "Characteristics and applications of biochar for environmental remediation: A review." *Crit. Rev. Env. Sci. Technol.* 45 (9): 939–969. https://doi.org/10.1080/10643389.2014.924180.
- Xu, Q., T. Townsend, and D. Reinhart. 2010. "Attenuation of hydrogen sulfide at construction and demolition debris landfills using alternative cover materials." Waste Manage. (Oxford) 30 (4): 660–666. https://doi.org/10.1016/j.wasman.2009.10.022.
- Yargicoglu, E. N., and K. R. Reddy. 2017a. "Effects of biochar and wood pellets amendments added to landfill cover soil on microbial methane oxidation: A laboratory column study." *J. Environ. Manage*. 193: 19–31. https://doi.org/10.1016/j.jenvman.2017.01.068.
- Yargicoglu, E. N., and K. R. Reddy. 2017b. "Microbial abundance and activity in biochar-amended landfill cover soils: Evidence from large-scale column and field experiments." *J. Environ. Eng.* 143 (9): 04017058. https://doi.org/10.1061/(ASCE)EE.1943-7870.0001254.
- Yargicoglu, E. N., and K. R. Reddy. 2018. "Biochar-amended soil cover for microbial methane oxidation: Effect of biochar amendment ratio and cover profile." *J. Geotech. Geoenviron. Eng.* 144 (3): 04017123. https://doi.org/10.1061/(ASCE)GT.1943-5606.0001845.
- Yargicoglu, E. N., B. Y. Sadasivam, K. R. Reddy, and K. Spokas. 2015. "Physical and chemical characterization of waste wood derived biochars." *Waste Manage. (Oxford)* 36: 256–268. https://doi.org/10.1016/j.wasman.2014.10.029.
- Yilmaz, D., L. Lassabatere, R. Angulo-Jaramillo, D. Deneele, and M. Legret. 2010. "Hydrodynamic characterization of basic oxygen furnace slag through an adapted BEST method." *Vadose Zone J.* 9 (1): 107–116. https://doi.org/10.2136/vzj2009.0039.
- Yilmaz, D., L. Lassabatere, D. Deneele, R. Angulo-Jaramillo, and M. Legret. 2013. "Influence of carbonation on the microstructure and hydraulic properties of a basic oxygen furnace slag." *Vadose Zone J.* 12 (2): vzj2012.0121. https://doi.org/10.2136/vzj2012.0121.